NUCLEAR MAGNETISM OF SOLID HELIUM-THREE

By

CHARLES VALENTINE BRITTON

A DISSERTATION PRESENTED TO THE GRADUATE COUNCIL OF
THE UNIVERSITY OF FLORIDA
IN PARTIAL FULFILLMENT OF THE REQUIREMENTS FOR THE
DEGREE OF DOCTOR OF PHILOSOPHY

UNIVERSITY OF FLORIDA

1977

To Rose
and Pat

ACKNOWLEDGMENTS

The author wishes to express his sincere appreciation to his advisor, Professor E. Dwight Adams, for his most helpful advice and encouragement during the course of this work.

Special thanks are due Dr. Donovan M. Bakalyar and Dr. Ephraim B. Flint for their participation in much of this work. The skillful machining and cheerful technical advise of William E. Steeger are gratefully acknowledged. Finally the author would like to express his heartfelt appreciation to his wife and daughter for their constant support through the years.

TABLE OF CONTENTS

Abstract of Dissertation Presented to the Graduate Council
of the University of Florida
in Partial Fulfillment of the Requirements
for the Degree of Doctor of Philosophy

NUCLEAR MAGNETISM OF SOLID
HELIUM-THREE

By

Charles Valentine Britton

December 1977

Chairman: E. Dwight Adams
Major Department: Physics

Nuclear magnetism in solid ^{3}He has been investigated through measurements of the exchange pressure in high magnetic fields and measurements of the magnetic susceptibility along the melting curve from 20 mK to temperatures approaching the ordering transition.

The field dependence of the exchange pressure has been accurately determined and the temperature dependence verified. From these measurements the value of the lowest order magnetic exchange parameter has been determined with increased accuracy.

The magnetic susceptibility has been measured along the melting curve. For temperatures above 4 mK the behavior can be expressed in the Curie-Weiss form with $\theta = -3.7$ mK. Below 4 mK however, the susceptibility rises abruptly to values approximately twice those of the Curie-Weiss law.

CHAPTER I

INTRODUCTION

The relative simplicity of solid ^{3}He has made it an attractive material for theoretical study and as low temperature techniques have accumulated to test theories and lay groundwork for new hypotheses.

The single, unpaired neutron in the ^{3}He nucleus gives rise to a nuclear spin I = 1/2 and a magnetic moment $\mu = 1.07 \times 10^{-26}$ J/T. The nuclear spin system is completely randomized at high temperatures, but as the thermal energy is decreased the spin interactions will begin to predominate and at some temperature T_c the solid will become magnetically ordered. The magnetic dipole interaction was considered by Pomeranchuk (1950) to produce an ordering temperature on the order of 10^{-7} K. However, there is another interaction in ^{3}He that is many times stronger than the magnetic dipole interaction. Bernandes and Primakoff (1960) showed that the quantum-mechanical exchange energy, which arises from antisymmetrizing the Fermi particle wavefunctions, is much larger in ^{3}He than in other materials. The small mass of the atom leads to a large zero-point motion and thus a large overlap of the atomic wavefunctions. This overlap is a measure of the exchange probability for neighboring atoms and gives the

exchange energy its high value. The estimates of Bernandes and Primakoff were shown to be considerably too high, but their work was the beginning of a great theoretical effort and a stimulus to experimental work already begun on exchange-related phenomena in solid ^{3}He.

During the ten years following the work of Bernandes and Primakoff a wide range of experiments produced data suggesting that an antiferromagnetic ordering of the nuclear spins would occur near 2 mK for the solid near melting pressure. These data were interpreted consistently by means of the Heisenberg Nearest-Neighbor (HNN) model (see next section) with rather small experimental errors involved.

The adequacy of the HNN model, however, was brought into doubt by measurements of the exchange pressure of solid ^{3}He in relatively high magnetic fields. The results of Kirk and Adams (1971, 1974) require an exchange constant smaller than previously deduced, by a factor of two. Several experiments since then have also revealed inconsistencies with the HNN model. An ordering of solid ^{3}He has actually been observed near 1 mK rather than 2 mK (Halperin et al., 1974; Kummer et al., 1975, 1977).

The discrepancy between the HNN model and the recent high-field data and low-temperature data has been the stimulus for many theoretical papers during the intervening years. However, at present, there is no simple model which is consistent with all the existing experimental data.

The experiments described in this dissertation were designed to provide further information on two of the previous areas of most basic conflict. Pressure measurements in high fields have been extended to somewhat lower temperatures and particular attention has been paid to determining, with increased precision, the field dependence of the data. The magnetic susceptibility of solid ^{3}He formed at melting pressure in a Pomeranchuk cell has been measured, using a pulsed NMR technique, down to temperatures approaching the ordering transition. Preliminary reports of this work have been made by Flint et al. (1977) and Bakalyar et al. (1977).

A Hamiltonian for Solid ^{3}He

As a basis for understanding current theories of exchange and for interpreting the results presented here, a generalized Hamiltonian will be presented.

The Hamiltonian for solid ^{3}He may be written as a sum of contributions from lattice vibrations (H_L), the magnetic dipole interaction (H_D), the exchange interaction (H_X), and the Zeeman energy in a magnetic field (H_Z),

$$H = H_L + H_D + H_X + H_Z \ . \qquad (1.1)$$

The characteristic temperature for lattice vibrations in solid ^{3}He is, $\theta_D \approx 20$ K and contributions from the phonons are negligible below 100 mK. As Pomeranchuk noted, the

magnetic dipole interaction will be important only in the μK region. In the temperature range between 1 mK and 100 mK only the exchange and Zeeman terms are relevant. Thus we have

$$H = H_X + H_Z \tag{1.2}$$

An early model for treating the exchange term is the Heisenberg Hamiltonian,

$$H_X = -2 \sum_{i<j} J_{ij} \vec{I}_i \cdot \vec{I}_j , \tag{1.3}$$

with the sum being over all pairs of spins in the system.

This treatment reduces the many-body Fermion problem to a sum over two-body spin interactions. The exchange energies J_{ij} are thus one half the difference in energy between the singlet state (antiparallel spins) and the triplet state (parallel spins) which are formed when the exchange interaction breaks the degeneracy of the ground state of the i^{th} and j^{th} spin 1/2 particles.

$$2J_{ij} = E_s - E_t \tag{1.4}$$

The Heisenberg Nearest Neighbor (HNN) model follows from Eqn. (1.3) by limiting the summation to first neighbors,

$$H_{nn} = -2J \sum_{i<j}^{nn} \vec{I}_i \cdot \vec{I}_j . \tag{1.5}$$

Since all lattice sites are equivalent, the constant J has replaced J_{ij} and has been removed from the summation.

In this approximation we see that the type of magnetic ordering expected as $kT \to |J|$ is determined by the sign of J. For $J>0$ the energy of the nearest neighbor pair is minimized by parallel spin alignment which would produce a ferromagnetically ordered solid, whereas for $J<0$ the energy of the pair is minimized by antiparallel spin alignment which would produce an antiferromagnetically ordered solid.

The magnitude of J determines the temperature at which the transition to the ordered state occurs, and the sign of J determines the nature of the ordered state.

When an external magnetic field is applied, consideration must be given to the Zeeman energy,

$$H_Z = \sum_i \vec{\mu}_i \cdot \vec{B} \tag{1.6}$$

where $\vec{\mu}_i$ is the magnetic moment of the i^{th} ^{3}He atom.

While the nearest neighbor pair exchange model was used for many years to describe consistently experimental properties of solid ^{3}He, recent results have shown it to be inadequate. Hamiltonians now being considered include some combination, or all, of the following,

i) pair exchange of nearest neighbors J_{nn},

ii) pair exchange of next nearest neighbors J_{nnn},

iii) pair exchange of third nearest neighbors J_{nnnn},

iv) triple exchange (around a triangle consisting of two nearest neighbor legs and one next-nearest neighbor leg) J_3,

v) quadruple exchange in a planar array (around a rhombus consisting of all nearest neighbor sides) J_{4P},

vi) quadruple exchange in a folded array (around a tetrahedron consisting of all nearest neighbor sides) J_{4F}.

Other triple and quadruple exchange processes are possible but calculations with the many-body wave functions indicate that the importance of terms not listed above can be neglected (McMahan and Guyer, 1973; McMahan and Wilkins, 1975).

Thermodynamic Quantities

Rather than specify which combination of exchange terms should be included in H_x, we shall consider a high temperature expansion of the partition function Z derived from an exchange Hamiltonian of undetermined form, plus the Zeeman Hamiltonian. This approach was suggested by McMahan (1974) and yields the expansion

$$\frac{1}{N} \ln Z = \frac{1}{N} \log \sum_{n=0}^{\infty} \frac{\text{Trace}(H_x+H_z)^n}{n!}$$

$$\equiv \ln 2 + \frac{3}{2}\beta^2 J_{xx}^2 - \frac{1}{2}\beta^3 J_{xxx}^3 + \ldots \qquad (1.7)$$

$$+ \frac{1}{2}(\beta\mu B)^2 [1 - 4\beta J_{xzz} + \ldots] + \frac{1}{12}(\beta\mu B)^4 [1 + \ldots,$$

where the moments of H_x are defined by

$$J^2_{xx} = \frac{\text{Trace } H_x H_x}{\text{Trace } H_1 H_1} , \tag{1.8}$$

$$J_{xzz} = \frac{\text{Trace } H_x H_z H_z}{\text{Trace } H_1 H_z H_z} , \tag{1.9}$$

$$\vdots$$

$$J^n_{x\ldots x\, z\ldots z} = \frac{\text{Trace } H_x \ldots H_x \; H_z \ldots H_z}{\text{Trace } H_1 \ldots H_1 \; H_z \ldots H_z} \tag{1.10}$$

(n factors of H_x, m factors of H_z in the numerator; n factors of H_1, m factors of H_z in the denominator)

with H_1 the Hamiltonian of a Heisenberg near neighbor magnet with exchange constant of magnitude 1. This normalization of the moments is such that if H_x is the Heisenberg nearest neighbor Hamiltonian, all the J's are equal and the expansion of Z is then equal to that derived by Baker et al. (1967) for the spin 1/2 HNN model. These workers give coefficients in the expansion of $\ell n\ Z$ up to 10 terms in $x = \beta J$ with $B=0$ and terms up to eighth order in x and $y = \beta\mu B$ for $B \neq 0$.

The various thermodynamic quantities of interest are found from Eqn. (1.7) as follows,

$$P(T,B) = \frac{N}{V} kT \left[\frac{3}{2} \gamma_{xx}^2 \beta^2 J_{xx}^2 - \frac{1}{2} \gamma_{xxx} \beta^3 J_{xxx}^3 + \ldots\right] + \frac{N}{V} \frac{(\beta\mu B)^2}{2} \left[4\gamma_{xzz} J_{xzz} + \ldots\right] \tag{1.11}$$

with

$$\gamma_{xx} = d(\ell n\ J_{xx}^2)/d(\ell n\ V)$$

$$\gamma_{xxx} = d(\ell n\ J_{xxx}^3)/d(\ell n\ V)$$

$$\gamma_{xzz} = d(\ell n\ J_{xzz})/d(\ell n\ V)$$

$$\chi = (kT/V)(\partial^2 \ell n\ Z/\partial^2 B^2)_{V,T}$$

$$= \frac{N\mu^2}{k\ TV}\ [1 + 4\beta J_{xzz} + 12\beta^2 J^2_{xxzz} + \ldots] \quad (1.12)$$

$$S = \frac{\partial}{\partial T}\ (kT\ \ell n\ Z)_{V,H}$$

$$\frac{S(T,B)}{Nk} = \ell n\ 2 - \frac{3}{2}\ \beta^2 J^2_{xx} + \beta^3 J^3_{xxx} - 1.325\beta^4 J^4_{xxxx} + \ldots$$

$$+ (\beta\mu B)^2\ [-4\beta J_{xzz} + \ldots] + \ldots \quad (1.13)$$

and

$$C_V = T(\frac{\partial S}{\partial T})_{V,H}$$

$$\frac{C(T,B)}{Nk} = 3\beta^2 J^2_{xx} - 3\beta^3 J^3_{xxx} + 5.30\beta^4 J^4_{xxxx} + \ldots$$

$$+ (\beta\mu B)^2\ [12\beta J_{xzz} - \ldots \quad (1.14)$$

The various J coefficients can be determined by fitting experimental data. Specific spin Hamiltonians can then be constructed which provide these J's through Eqn. (1.10).

Early Exchange Measurements
HNN Model

The original treatment of exchange in solid ^{3}He was based on the one parameter Heisenberg Nearest Neighbor approximation which consists of all the J's in Eqn. (1.7) being equal. The first properties to be measured which displayed exchange effects were spin diffusion and relaxation.

NMR measurements of these dynamic processes were possible at temperatures as high as 1K. The analysis required to extract values of J from these measurements however, is not straightforward and the results of even high-precision measurements have not always been consistent. These high-temperature NMR experiments are reviewed by Guyer et al. (1971) and are not considered further here.

With lower temperatures becoming more readily available, considerable improvements in the precision of J measurements have occurred through observations of various thermal equilibrium properties. The exchange dependence of these measurements is subject to a much more direct interpretation than of the early NMR measurements.

The first thermodynamic determinations of $|J|$ were by Panczyk et al. (1967) and by Panczyk and Adams (1969) using high resolution pressure measurements at constant molar volume. A range of molar volumes, covering most of the bcc phase were used, allowing the volume dependence of $|J|$ to be measured as well as $|J|$ itself. The results of Panczyk et al. are shown in Figure 1, where $\Delta P = P_V(T) - P_o$ with P_o determined by extrapolating the 1/T dependence such that $P(1/T = 0) = P_o$. The agreement of this data with the expression in Eqn. (1.11) is quite good. The contribution of the J^3 term produces a deviation from the 1/T dependence of only 2% at the lowest temperatures and is not large enough to determine the sign of J. In these measurements B=0.

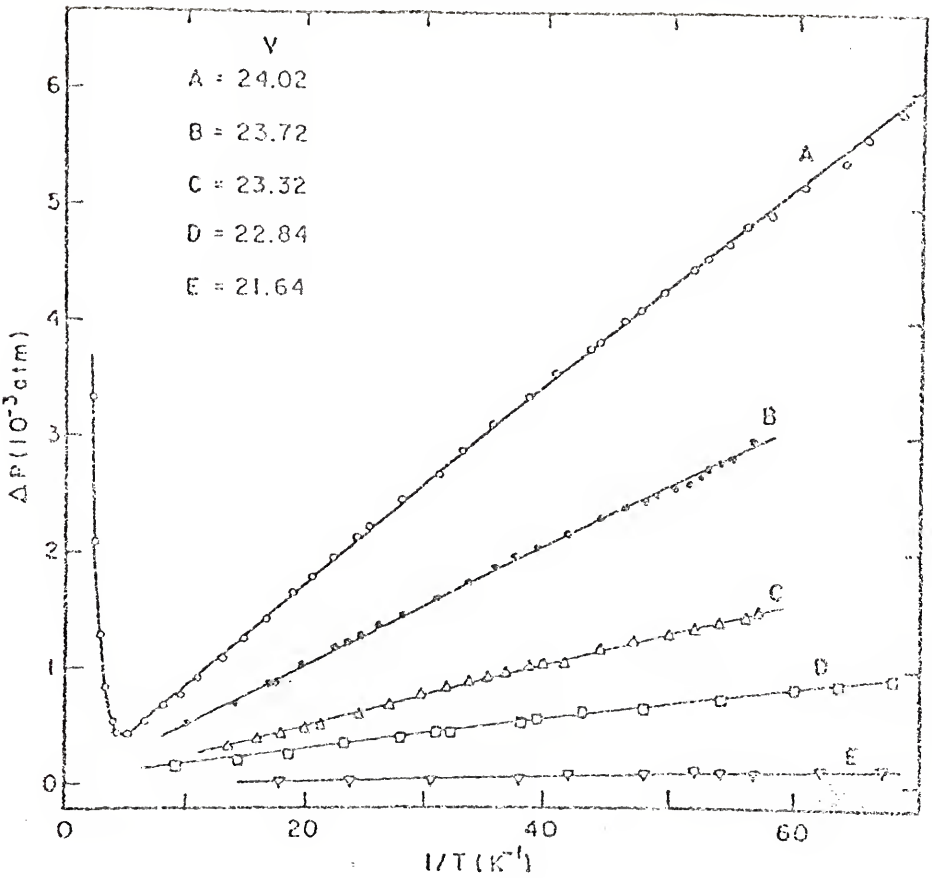

Fig. 1 Zero-Field Pressure Measurements. Pressure difference ΔP [$= P_V(T) - P_o$] versus T^{-1} for various molar volumes. For $v = 24.02$ cm^3/mole the high temperature phonon contribution is shown; for the other volumes only the exchange contribution is shown. (Note: 1 atm = 101.3 kPa.) (After Panczyk and Adams, 1969.)

Magnetic susceptibility measurements are able to determine the sign of J however. The measurements of Kirk et al. (1969) covered a wide range of molar volumes in the bcc phase and are shown in Figure 2. The data are often interpreted in the Curie-Weiss form. Taking the first two terms of Eqn. (1.12), setting $\theta = 4J/k$, we have

$$\chi = C/(T - \theta) \tag{1.15}$$

for $T \gg \theta$. The results of Kirk et al. show clearly that θ (hence J) is negative, indicating antiferromagnetic ordering. The magnitudes of J found in this work are consistent with those taken from $P_V(T)$ but their precision is considerably lower than that of the pressure measurements.

The computations of Baker et al. (1967) for the HNN model show that the ordering temperature $T_N = -2.748\ J/k = -0.6870\theta$. The magnetic susceptibility data and the pressure data in zero field indicated that the transition to an antiferromagnetically ordered phase would be expected to occur at $T_N \cong 2.0$ mK for a solid sample near melting pressure ($V_m = 24.1\ cm^3/mole$).

More recently, the specific heat of bcc ^{3}He has been measured by Castles and Adams (1973, 1975), by Dundon and Goodkind (1974) and by Graywall (1977) to sufficiently low temperatures to extract the exchange contribution. Except for the results of Dundon and Goodkind, the values of J found in the measurements are in excellent agreement with those found in the zero-field pressure and magnetic

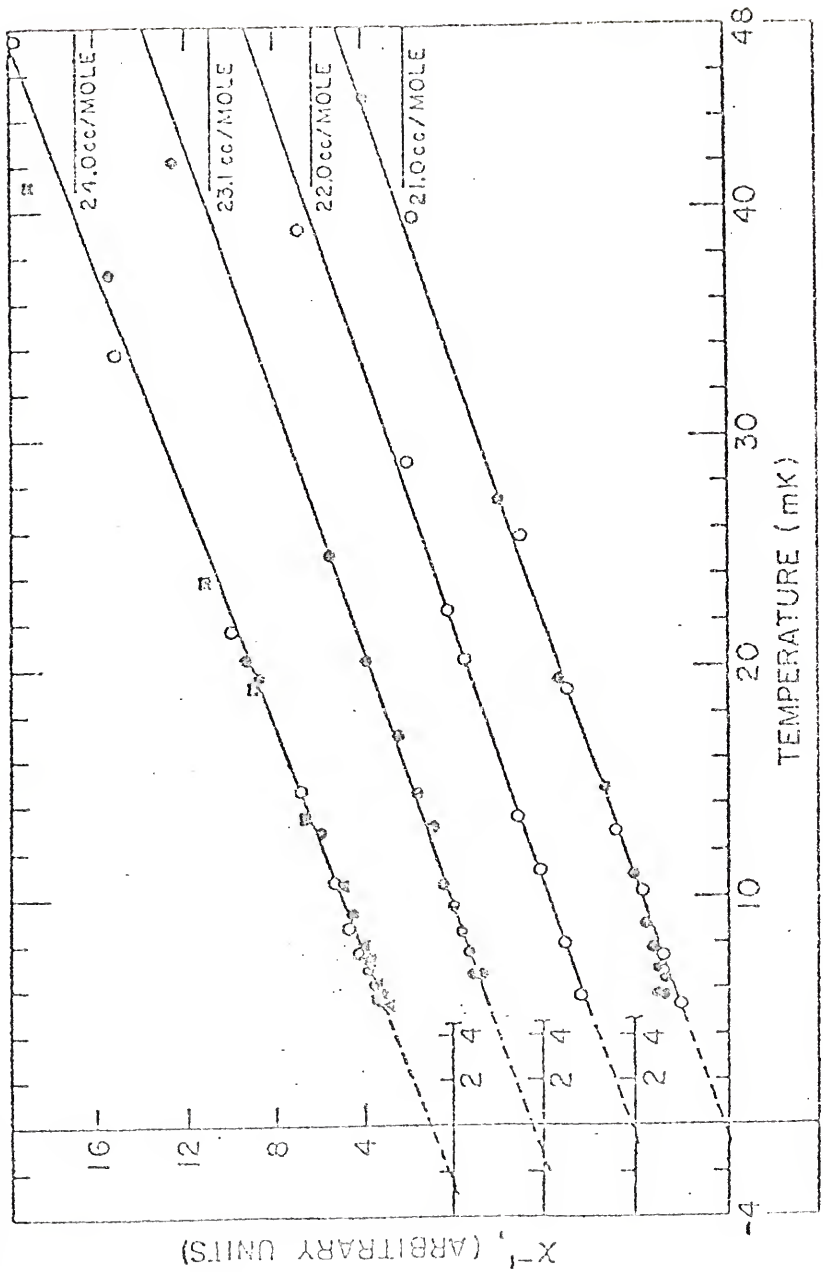

Fig. 2 Susceptibility Measurements. Inverse susceptibility versus temperature for various molar volumes. (After Kirk et al., 1969.)

susceptibility measurements. These results are summarized in Figure 3 (after Greywall, 1977). This figure illustrates how consistently the one parameter HNN model was able to describe the specific heat, pressure and magnetic susceptibility.

Failure of the HNN Model

The first evidence that the HNN model was inadequate in describing the properties of solid ^{3}He was provided by the pressure measurements of Kirk and Adams (1971,1974) done in moderately high magnetic fields. The effect of an externally applied magnetic field may be seen from Eqn. (1.11). The first term involving the magnetic field dependence contains the factors $\beta^2 B^2 J_{xzz}$. The departure from 1/T dependence of the pressure in a magnetic field will thus show the sign of J and the variation with the strength of the magnetic field should show the magnitude. The results of Kirk and Adams for a sample of molar volume 23.34 cm^3/mole are shown in Figure 4. The data do show a qualitative agreement with the HNN model calculation and do show J to be negative. The magnitude of pressure change caused by the magnetic field however, is only 60% as great as that expected, based on calculations using J values measured in previous experiments. Higher order terms are not capable of reducing this discrepancy and the differences involved are many times larger than the experimental uncertainties.

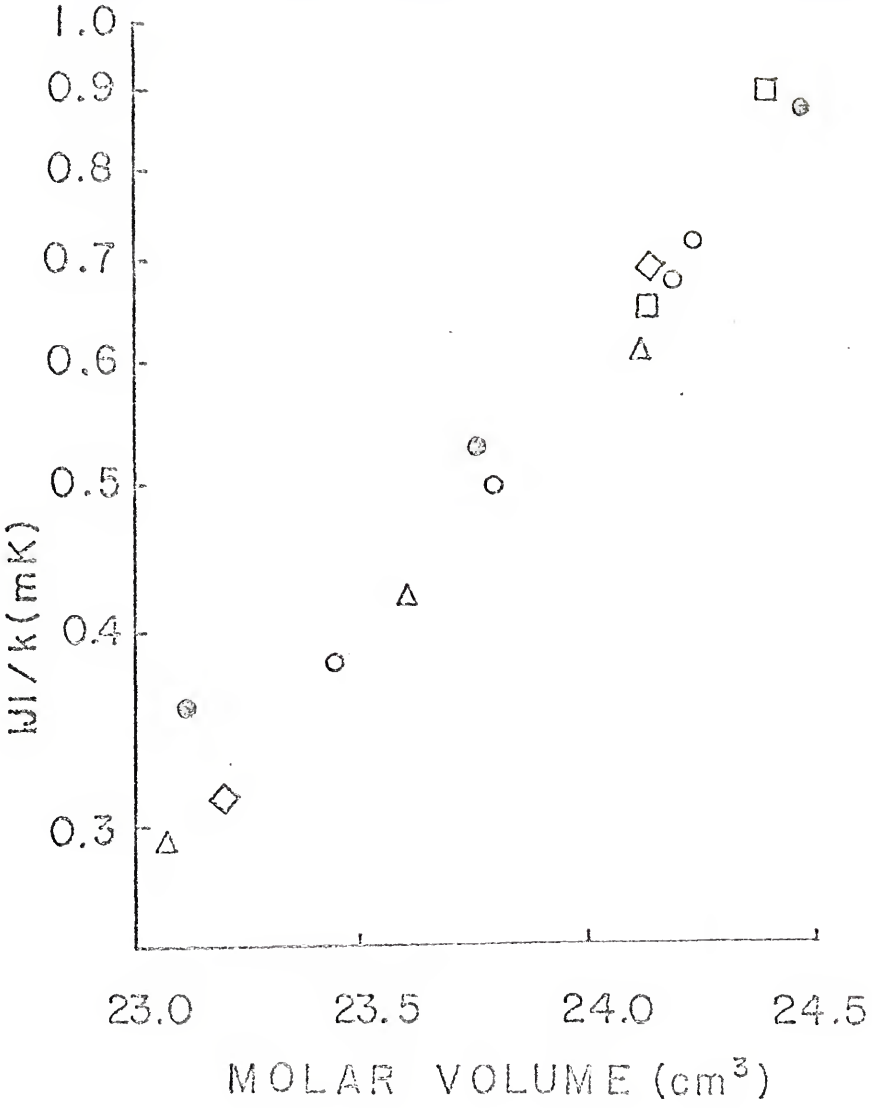

Fig. 3 HNN J's collected from the literature.
(After Greywall, 1977.)

(⊙) Greywall, 1977; (□) Castles and Adams, 1973,1975;
(◇) Kirk et al., 1969; (○) Panczyk and Adams, 1969;
(△) Richardson et al., 1965.

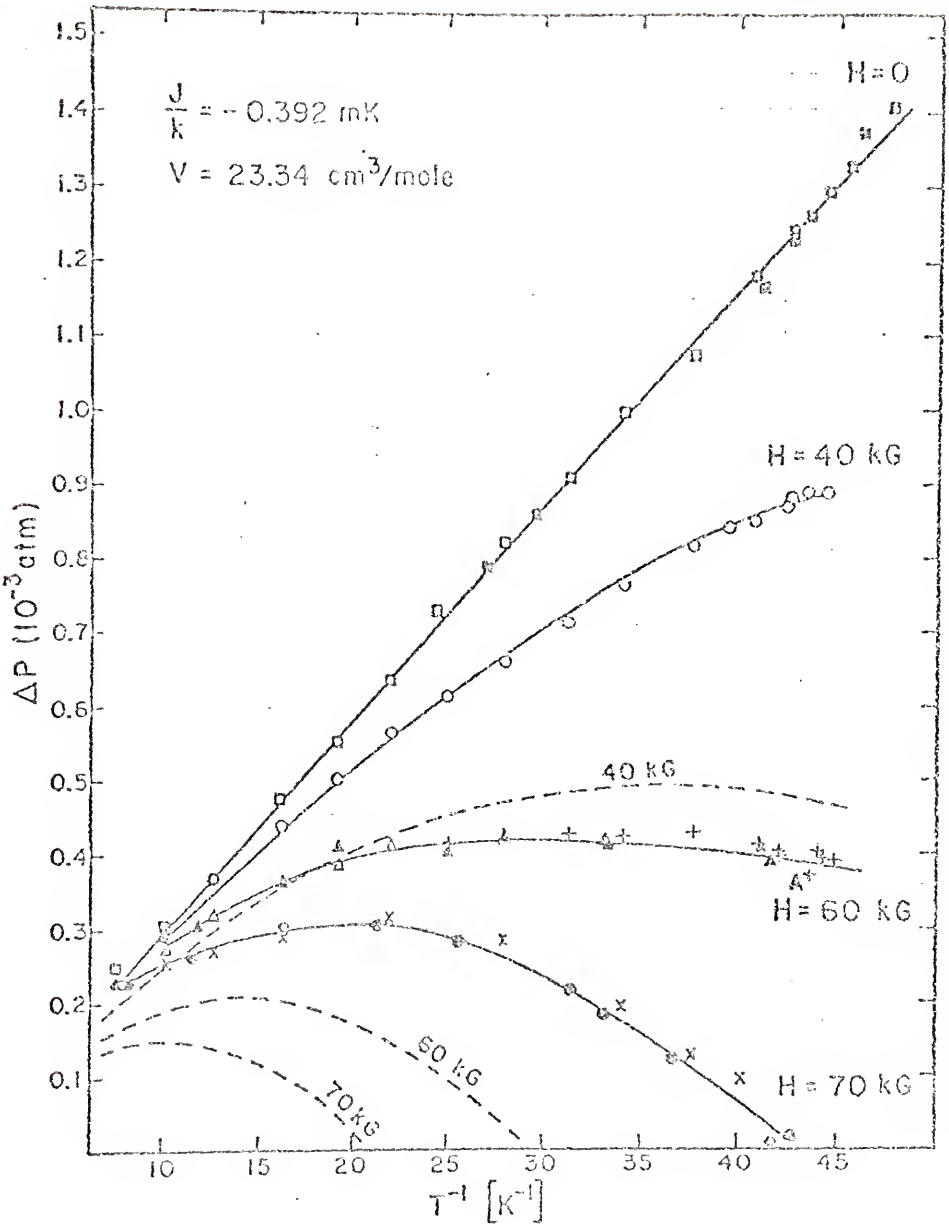

Fig. 4 High-Field Pressure Measurements. Pressure difference versus T^{-1} for $v = 23.34$ cm³/mole in several magnetic fields. The dashed curves show the calculated behavior based on the HNN model, equation (1.11). (Note: H = B; 1 kG = 0.1 T; 1 atm = 101.3 kPa.) (After Kirk and Adams, 1971.)

Measurements of the ^{3}He melting curve by Osheroff et al. (1972) indicated that the expected magnetic ordering had not occurred at temperatures well below 2 mK. The melting curve was expected to become quite flat in the region of the solid ordering (with a maximum occurring if the solid molar entropy has become equal to the liquid molar entropy), but Osheroff et al. found the pressure still to be rising at temperatures well below 2 mK.

The ordering of the solid has now actually been observed by Halperin et al. (1974), Dundon and Goodkind (1974) and by Kummer et al. (1975, 1977). These experiments observe a rapid decrease in the entropy of the solid at a temperature of 1.1 mK rather than 2 mK as expected from the HNN model.

Summary and Objective

A summary of the experiments just discussed is given in Table 1 with the various J values determined by fitting Eqn. (1.7) to the experimental data. This compilation is due to McMahan (1974) and Halperin (1977). The molar volumes of each experiment have been scaled to 24.14 cm^3/mole, assuming that each J is proportional to v^{18}.

The necessity of going beyond the HNN model to explain the experiments done at high fields and those done at low temperatures is obvious but the ability of any more generalized spin interaction Hamiltonian to describe solid ^{3}He must be based on consistent values for the moments of the Hamiltonian as listed in Table 1. The values shown in column one

Table 1.

Moments of the Hamiltonian in the notation of McMahan.
(After McMahan, 1972 and Halperin, 1977)

Measurement	J_{xzz}/k_B (mK)	$\lvert J_{xx}\rvert/k_B$ (mK)	J_{xxx}/k_B (mK)	Reference
X(T)	-.7±.2			Kirk et al. (1967)
P(T,B=0)		.66±.02		Panczyk and Adams (1969)
P(T,B≠0)	-.33±.07			Kirk and Adams (1971,1974)
C(T)		.67±.07		Castles and Adams (1973,1975)
C(T)		.83±.08	1.04	Dundon and Goodkind (1974)
C(T)		.700±.003		Greywall (1977)
S(T)		.95±.12	1.11±.25	Halperin (1975 a,b)
S(T)		1.15		Kummer (1975,1977)

and two show that experiments which in principle are determining the same quantities, yield values differing by as much as a factor of two. If these experiments cannot be reconciled, the entire notion of a spin-interaction Hamiltonian may have to be discarded.

The discrepancy shown in the J_{xzz} column of Table 1 is our concern here. These values of the first magnetic exchange coefficient are derived from magnetic susceptibilities in the first instance and from pressure measurements in the second. The three independent sets of susceptibility measurements which are the basis for the first entry in column one were reported by Kirk et al. (1969), Sites et al. (1969), Pipes and Fairbank (1969), and Bernat and Cohen (1973). Determining the Weiss theta (which determines J_{xzz} through Eqns. (1.12) and (1.15)) requires extrapolating from a sometimes quite high temperature and great care must be taken that curvature produced by higher order J's in Eqn. (1.12) does not lead to an overestimate of $|\theta|$. Sites et al. and Kirk et al. took steps in their analysis to avoid errors owing to curvature. These two sets of data claim the smallest error bars of the current measurements and their values for θ at melting pressure are in good agreement. Their analysis would make it appear unlikely that their values of J_{xzz} is overestimates by any amount approaching the factor of two required to reconcile it with that from the pressure measurements done in a magnetic field.

The resolution of the pressure measurements of Kirk and Adams should inherently be superior to that of the susceptibility measurements. The sensitivity of the gauge employed by them was 2×10^{-6} atm while pressure changes caused by the applied field were as large as 2×10^{-3} atm. The high precision of the pressure measurements is somewhat clouded by the field dependence of the pressure. As pointed out by Goldstein (1973) the pressure change due to the applied field should, for thermodynamic reasons, be proportional to the square of the applied field strength. The data of Kirk and Adams show what seem to be random variations from this behavior, approaching 20% in one instance.

The present work was undertaken in an effort to remove some of the uncertainty surrounding the high field pressure measurements, and to determine the magnetic susceptibility of solid ^{3}He in the temperature range approaching the ordered phase.

CHAPTER II

APPARATUS

High Field Pressure Cell

A major difficulty present in studying low temperature properties of bulk solids is that of thermally coupling the solid material to the source of cooling and also of achieving a uniform temperature throughout the sample. The Kapitza thermal boundary resistance between solid helium and the surface of the cell increases as $1/T^3$ as the temperature is lowered, and the thermal conductivity of the solid decreases as T^3 as the temperature is reduced. Hence it is ncessary to construct an experimental cell with a large surface area to maximize the thermal contact with the solid, and also to limit the maximum dimension of the solid to allow all portions to reach thermal equilibrium in a reasonable length of time.

With these conditions in mind a sample chamber was designed as shown schematically in Figure 5. The upper portion of the cell was constructed of oxygen-free high conductivity (OFHC) copper. This copper section is thermally anchored to the mixing chamber of a ^3He-^4He dilution refrigerator by means of well annealed heavy copper wires. To provide thermal contact with the solid, a brush of approximately

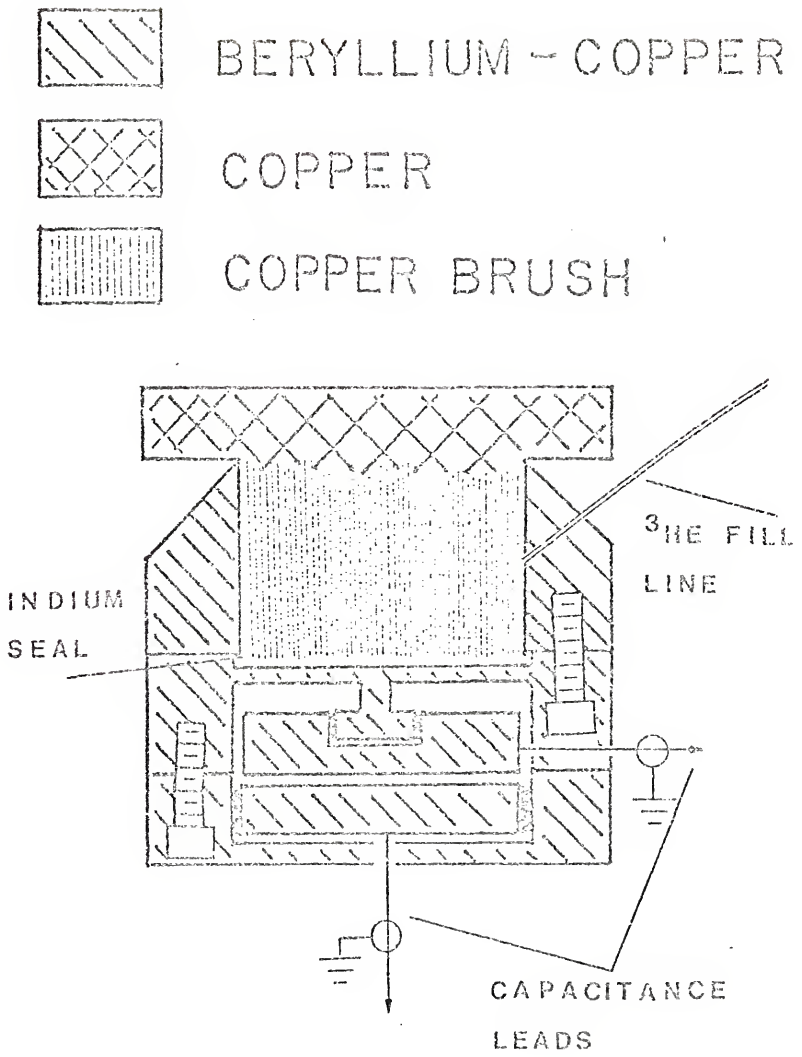

Fig. 5 High Field Pressure Cell.

$2x10^5$ Cu wires 0.025 mm in diameter was welded to the body of the cell. The lower portion of the cell consists of a capacitive strain gauge similar to those described by Straty and Adams (1969).

The active element of the strain gauge is the beryllium-copper (Be-Cu) diaphragm 1.07 mm thick and 24.4 mm in diameter which forms the lower surface of the sample chamber. The center of this diaphragm was epoxied to, but insulated from, the movable plate of a parallel plate capacitor. The strength of the sample chamber diaphragm is sufficient to withstand the working pressure greater than 5 MPa and produces a deflection of $25x10^{-12}$ m/Pa. A second diaphragm assembly was constructed, identical to the first except for the thickness of the diaphragm having been doubled. Use of this less flexible diaphragm will be discussed later.

The bridge circuit used in making the high resolution capacitance measurements is diagrammed in Figure 6. The reference capacitor is a silvered mica capacitor mounted on the still flange of the dilution refrigerator to minimize thermal drift. An Optimation 1100 signal generator is used to drive the General Radio 1493 Precision Decade Transformer and to provide the reference signal to the Keithley 840 lock-in amplifier. Seven decades of the ratio transformer were used and an eighth digit was interpolated from the output signal of the lock-in detector as displayed on a strip-chart recorder. With this resolution we were able to detect diaphragm displacements as small as $5x10^{-12}$ meter, corresponding to pressure changes of 0.2 Pa.

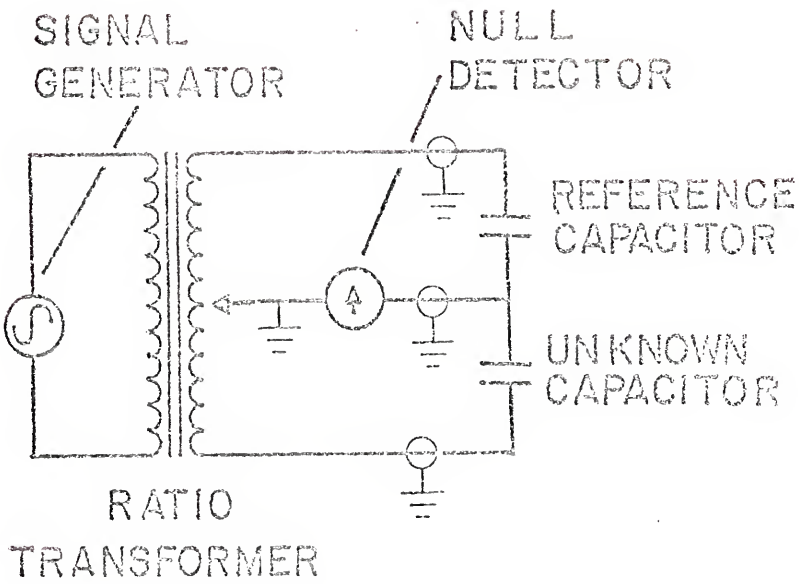

Fig. 6 Capacitance Bridge.

A "dipstick" of approximately 10 cm^3 volume, filled with activated charcoal, was used to condense ^3He from the storage bottle and to produce the necessary pressures within the cell. External pressures were measured with a Heise gauge which covers the pressure range of interest here.

Carbon thermometers, calibrated against the ^3He melting curve during the same run, were used to determine the sample temperature. Speer carbon composition resistors, nominally 100 ohms, were ground flat on two sides to expose the carbon core. The two surfaces were glued in close contact with a copper heat sink, taking care to avoid electrical contact. These thermometers were thermally linked to the sample cell and located outside the high magnetic field region. One such thermometer was mounted within an Nb_3Sn superconducting cylinder capable of excluding magnetic fields of 2.5 T. This thermometer should be free of any magneto-resistive effects which can cause large errors in thermometry.

Magnetic fields were generated by a superconducting solenoid capable of operating in a persistent mode. Field strengths were determined from the current using data provided by the manufacturer.

Low Temperature Susceptibility Cell

The magnetic susceptibility measurements were made in a Pomeranchuk cell, a modification of that used by Kummer et al. (1975,1976). The problem of producing solid ^3He at temperatures approaching 1 mK is solved by freezing the required

solid from the liquid while holding the temperature of the system constant. Thermal equilibrium within the solid is achieved by limiting the thickness of the solid layer formed.

The NMR region of the Pomeranchuk cell is shown in Figure 7. The tail-piece, filled with liquid and solid ^{3}He was machined from Epibond 100A thermosetting epoxy resin. The NMR radio frequency coil was wound around this epoxy chamber. In one set of measurements the rf coil was wound in a sixth-order compensated geometry onto a nylon cylinder which was slipped over the epoxy extension. The second set of measurements utilized a simple solenoid wound directly on the epoxy with the addition of a small counter-wound length to cancel the rf field just above the sample region.

The static magnetic field is produced by a Helmholtz pair of superconducting coils, mounted in the helium bath and operated in a persistent mode.

A pulsed NMR spectrometer (Instruments of Technology PLM-3) is used to measure the magnetization of the ^{3}He within the rf coil. The output of the PLM-3 is fed into a Fabri Tek 1062 signal averager which has a digital printer to record the averaged signal.

A resistivity heater is distributed uniformly throughout the experimental region providing the surface on which the solid ^{3}He is formed. The Heater consists of a 300 m length of 92% Pt, 8% W alloy wire, 0.023 mm in diameter, wound noninductively on a spool centered within the rf coil. The double windings of the heater are spaced 0.15 mm apart

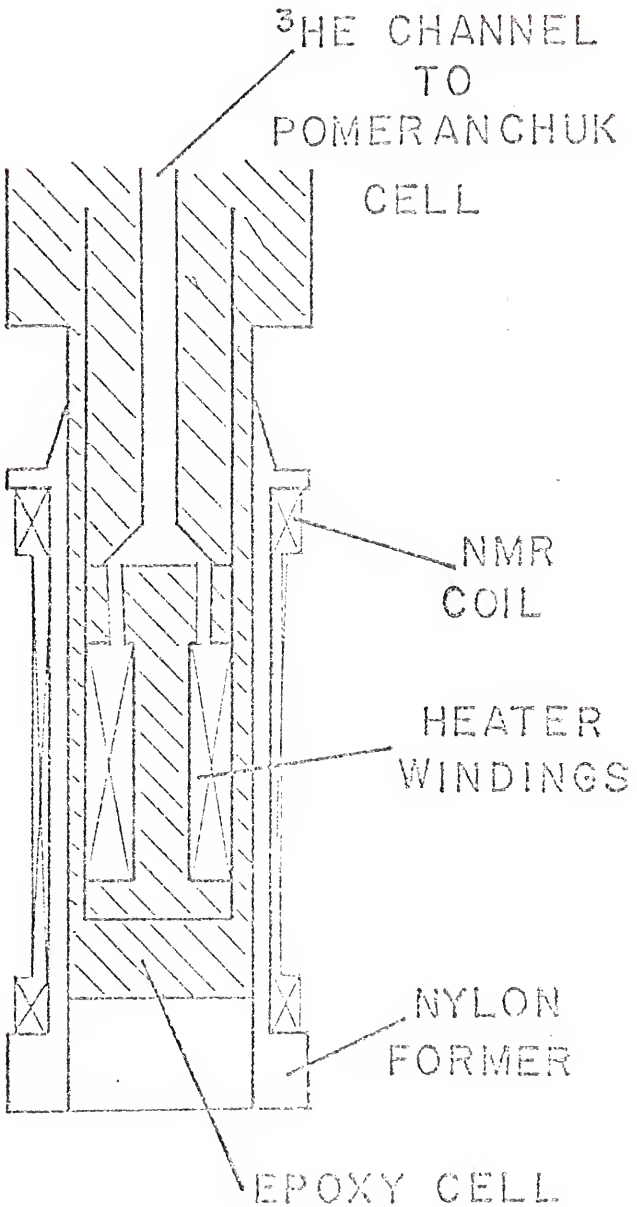

Fig. 7 NMR Region of Susceptibility Cell.

and each of the 50 layers of wire is separated from the adjacent layers by a layer of tissue paper 0.076 mm thick. This heater provides a surface area of 220 cm^2 so that the layer of solid formed will be quite thin. The volume of solid formed in a typical heat pulse is 24 mm^3, producing a layer of solid only 1 μm in thickness. This assures that the thermal time constant for returning to equilibrium will be short (less that 10 sec.).

Pressures of the ^3He and ^4He are measured with capacitive strain gauges of the type described previously. The gauge which measures the ^3He pressure is mounted within the Pomeranchuk cell body. The ^4He gauge is mounted on the mixing chamber flange of the dilution refrigerator. The ^4He pressure is always less than that required to form solid ^4He so this gauge will give an accurate indication of the ^4He pressure in the cell. The capacitance of the ^3He gauge is measured with a General Radio 1615-A capacitance bridge with an Ithaco 391A lock-in detector. The ^4He capacitance is measured using a ratio transformer and a reference capacitor mounted on the still flange of the dilution refrigerator. The off-balance signal from each capacitance measurement is recorded on a dual-trace chart recorder.

During the course of a magnetization measurement the ^3He pressure must be held constant. This is done through use of the feedback regulation system illustrated in Figure 8. The ^3He capacitance bridge is balanced at the desired pressure, and any error signal from the lock-in detector is amplified

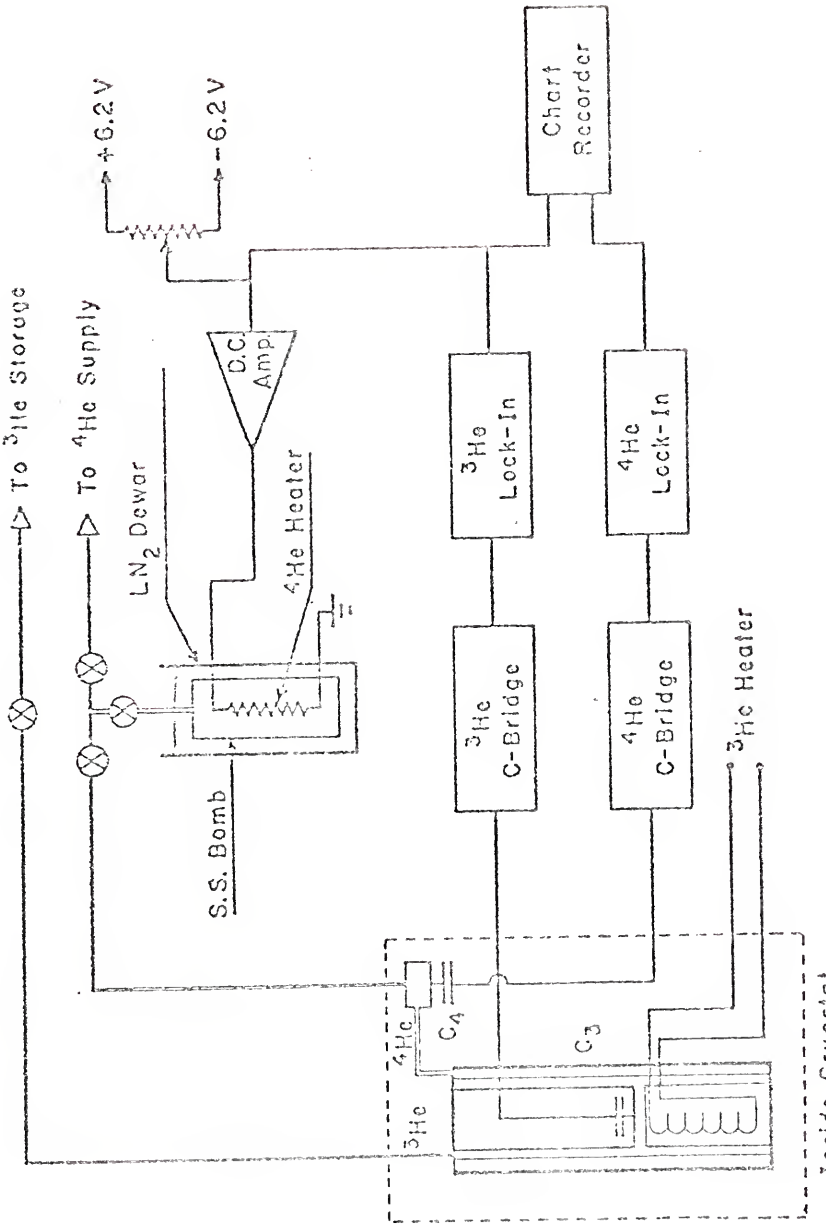

Fig. 8 ^{3}He Pressure Controller.

by the Kepco BOP36-5 operational power supply which adjusts the current in the ^{4}He pressure bomb, thereby compressing or decompressing the Pomeranchuk cell as required.

CHAPTER III

PROCEDURE

Pressure Measurements

Prior to forming the solid sample of ^{3}He, it was necessary to calibrate the capacitive strain gauge and also the resistors which would serve as thermometers during the actual data-taking. While the entire refrigerator was maintained at approximately 1K (by pumping on the ^{4}He cold plate evaporator), ^{3}He was condensed into the cell and pressurized using the charcoal filled dipstick. The strain gauge was calibrated against the Heise gauge in the external plumbing, covering a range in pressure from 3 MPa to 5 MPa. The ratio transformer reading R was related to the pressure P through the equation

$$P = a + b/(R + \Delta R) \tag{3.1}$$

using a least-squares fitting routine. The small correction ΔR was varied to minimize the rms deviation between the data and the fitted curve. The ratio $\Delta R/R$ is usually found to be about 10^{-2}. The term ΔR can be considered to result from the fringing field at the edge of the capacitor plates and/or stray capacitance in the other parts of the circuit.

Having calibrated the sample cell pressure gauge, a melting curve sample was formed. At a temperature of 1K the liquid pressure was set at 3.37 MPa and the sample line to the external plumbing was closed. The dilution refrigerator circulation was begun and the sample cooled. The pressure remained quite constant until the melting curve was reached at about 0.75 K. Below this temperature solid forms as more cooling occurs and the pressure drops. The minimum pressure P_{min} is reached at 0.32 K. The strain gauge reading corresponding to P_{min} is found by passing through the minimum in each direction. The coefficient "a" in Eqn. (3.1) is adjusted so that the minimum reading yields a pressure of 2.9316 MPa which is the accepted value of P_{min}. This small correction usually amounts to less than 0.01 MPa.

The ^{3}He in the cell will consist of both solid and liquid down to the lowest temperatures reached in these measurements (less than 15 mK). As the cell cools below 0.32 K solid ^{3}He melts (because of its negative latent heat) and the pressure rises. The various thermometers are calibrated by maintaining a constant resistance (i.e., temperature) and measuring the pressure in the cell. Values of the melting pressure as a function of temperature are used as tabulated by Trickey et al. (1972).

To form an all solid sample of large molar volume, the cell must be warmed above the pressure minimum so that the sample capillary will not be blocked by solid. The liquid pressure in this case was then raised to 4.7 MPa and the

cell allowed to cool. At 1.25 K the melting curve was reached and solid began to form in the cell. The pressure dropped rapidly as the melting curve was followed toward the minimum. At 0.89 K the sample was completely solidified and the pressure change slows dramatically. By noting the temperature at which the solid left the melting curve the molar volume can be determined. In this case the all solid pressure was 3.66 MPa, the melting curve was left at 0.89 K, indicating a molar volume of 23.96 cm^3/mole. The solid was annealed for about one hour at a temperature about 10 mK below the melting curve, to relieve internal pressure gradients. Once the annealing process was completed, further temperature changes were made slowly.

Temperature intervals were chosen equally spaced in 1/T covering temperatures from 150 mK to 15 mK. Having completed pressure measurements over the entire temperature range the magnetic field was changed and the procedure repeated. It was found that the bulk pressure reading changed slightly when the magnetic field was changed. This may be because of some helium slipping into or out of the cell as a result of the warming that accompanied the rather rapid change of field. When plotting $\Delta P = P(T) - P_o$ versus 1/T a value of P_o was chosen such that the curve would extrapolate to $\Delta P = 0$ at $1/T = 0$.

The pressures measured as a function of temperature with this diaphragm were found to be about a factor of three lower than those found in previous investigations. It was suspected

that the helium contained within the wire brush might be frozen in place and not able to move and affect the pressure measured below the brush.[1] If this volume of helium were not taking part in the pressure changes, it would be possible that the small volume change associated with the diaphragm movement would be sufficient to substantially lower the pressure measured. To determine the volume of helium that was actually producing the pressure changes, the second diaphragm, having twice the thickness of the first, was used in repeating the measurement in zero magnetic field.

To account for pressure changes caused by volume change associated with diaphragm motion we consider P to be a function of T and V and write

$$\left(\frac{\partial P}{\partial T}\right)_V = \frac{dP}{dT}\left[1 + \frac{1}{K_T V}\frac{dV}{dP}\right] . \qquad (3.2)$$

By comparing the pressure measurements in zero field made with the two diaphragms of differing stiffness we are able to evaluate the correction factor necessary to convert our pressure data to truly volume independent results.

From the pressure-capacitance calibrations of the two diaphragms we are able to determine the volume-pressure behavior of each. The thicker diaphragm is 6.61 times stiffer; hence the volume change for a given pressure is 6.61 times less than that for the thinner diaphragm. Using the dP/dT values for the two measurements and values of the isothermal compressibility (Straty and Adams, 1967) we see that the volume

V of solid helium which is producing the pressure behavior is only 0.041 cm^3. This corresponds to the free volume in the cell below the wire brush. Although the volume of the cell is measured to be 1.38 cm^3, the volume of solid which is among the wires is evidently frozen in the narrow channels and is not able to affect the pressure measured below the brush.

For the more flexible diaphragm the quantity $\frac{1}{k_T V}\frac{dV}{dP}$ is equal to 1.50, so the constant volume pressure values are 2.50 times larger than the pressures measured.

Magnetization Measurements

The magnetization measurements are performed in a Pomeranchuk cell which produces cooling by compression of a liquid solid mixture of ^3He, with the formation of solid accompanied by the absorption of thermal energy. (The latent heat of fusion for ^3He is negative in the temperature interval from 1 mK to 320 mK.) Since, in the cooling process, the cell will always contain a mixture of liquid and solid, the melting pressure can be used for thermometry.

While the entire refrigerator is at a temperature of 1K, the two chambers of the cell are filled with ^3He and ^4He. A pressure-capacitance calibration is done for each fluid using external pressure gauges. The ^4He pressures include values up to 2.5 MPa. The ^3He pressures cover a pressure range of 2.8 MPa to 3.4 MPa (this being the change in pressure along the melting curve below 320 mK). The ^3He pressure is then

set at 3.24 MPa and the cell is quickly cooled below the minimum, thus sealing a sample of ^{3}He in the cell with a molar volume such that it will be entirely melted at a temperature near 25 mK. Two days of cooling is necessary to lower the temperature to this range.

When the liquid in the Pomeranchuk cell has cooled to about 15 mK, a trial compression is made to locate the transition to the superfluid A phase. A small additive correction (about 0.3%) is made to the pressure calibration so that the A transition which occurs at 2.75 mK corresponds to 3.4344 MPa as reported by Halperin et al. (1974). Other temperatures are measured relative to this pressure using the melting curve data of Halperin et al. and of Kummer et al. (1975, 1976).[2].

The magnetization of the ^{3}He within the NMR coil is measured by analyzing the free-induction-decay (FID) following 250 kHz pulses. Each pulse lasts 160 μsec; a delay of 320 μsec is allowed for the transmitter pulse to decay; then the FID of the nuclear spins is recorded by the Fabri Tek signal averager. Sixteen such pulses are averaged for a given measurement, and the FID is extrapolated back to the center of the applied pulse.

When the temperature at which a magnetization measurement is to be made is reached, the ^{3}He pressure is held constant by automatically controlling the ^{4}He compression rate using the feedback mechanism described previously. When the heat-leak into the cell appears to be constant (as

evidenced by a linear increase of ^{4}He pressure with time), a series of four magnetization measurements, spaced at one minute invervals, is made. Following the measurements a current pulse is applied to the heater within the NMR coil, forming a controlled volume of new solid on the surface of the heater wire. During this heat pulse the ^{3}He pressure is maintained constant, and the change in ^{4}He pressure as recorded on the chart output is a measure of the cell volume change and hence is proportional to the amount of new solid formed. A series of magnetization measurements is then made following the heat pulse. A typical sequence is illustrated in Figure 9. The magnetization values before the heat pulse and those after the heat pulse are least-square-fitted to linear functions and extrapolated to the center of the heat pulse. The difference between the two extrapolations is ΔM, the magnetization of the new solid formed (subject to a small correction for the liquid magnetization to be discussed later). The change in ^{4}He pressure (also measured at the center of the heat pulse) is proportional to the change in cell volume and hence to the volume of solid formed by the pulse. Thus the susceptibility of the solid at this temperature is $\chi \equiv \Delta M/\Delta V$ measured in arbitrary units.

The increase in magnetization measured after the heat pulse is actually the magnetization of the solid produced, less the magnetization of the equal volume of liquid which has been excluded by the solid formed. Thus, the susceptibility of the solid is given by

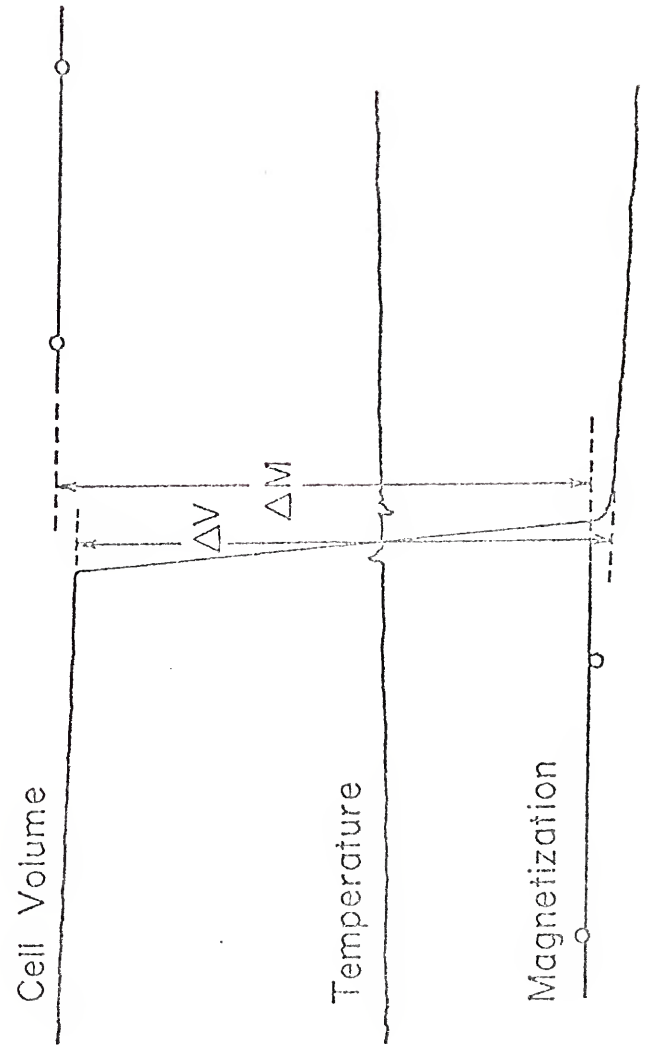

Fig. 9 Typical Chart Recordings of Cell Volume and Temperature with magnetization measurements superimposed.

$$\chi_S = \frac{\Delta M}{\Delta V} + \chi_L. \tag{3.3}$$

The subscripts S and L refer to solid and liquid respectively and the susceptibilities are expressed in the same arbitrary units. The liquid susceptibility χ_L is constant at these temperatures (if the very slight pressure dependence is ignored). At pressures near solidification χ_L is found (Ramm, et al., 1970) to be equal to the Curie value expected at 180 mK. For temperatures above 5 mK the solid follows the Curie-Weiss law so we have

$$\chi_L = \frac{C_L}{180} = \text{constant}$$

$$\chi_S = \frac{C_S}{T-\theta} \tag{3.4}$$

where C_L and C_S are the Curie constants and the temperatures are measured in mK. Then,

$$\frac{\chi_S}{\chi_L} = \frac{C_S}{C_L}\,\frac{180}{T-\theta} = \frac{V_L}{V_S}\,\frac{180}{T-\theta} \tag{3.5}$$

where V_L and V_S are the molar volumes of the liquid and solid at melting pressure.

From Eqns. (3.4) and (3.5) we have

$$\chi_L = \frac{\Delta M}{\Delta V}\left\{\frac{V_L}{V_S}\,\frac{180}{T-\theta} - 1\right\}^{-1}$$

which can be evaluated using our $\Delta M/\Delta V$ values, yielding the constant correction term χ_L which is to be substituted into

Eqn. (3.3). When the liquid becomes superfluid in the A phase, the liquid resonance is shifted away from the solid resonance frequency and the correction is not applicable.

In the early stages of these runs it was noticed that on some occasions when several heat pulses were applied a large scatter in the data was seen. After two or three pulses, subsequent measurements of χ would yield values consistently lower than those recorded in the first few measurements during a given compression. This behavior was most noticeable at temperatures above 5 mK. These anomalously low values of χ could be explained in two possible ways. If a part of the heat pulse were conducted out of the NMR region, the amount of solid seen in the magnetization measurement would be less than that recorded by the ^{4}He pressure change and the resulting χ value would be low. Alternatively a portion of the heater could become heavily coated with solid following a number of heat pulses and this region would not be in good thermal contact with the liquid in the cell. The solid in such an isolated region would remain hot following a heat pulse and hence cause a low measurement to be made.

To alleviate this problem only a few small heat pulses were used during the latter compressions. From an accumulation of data at a given temperature, those yielding the largest susceptibilities were taken as correct.

During one compression a different technique was used. After compressing to 2.5 mK and recording the usual initial

series of background magnetizations, heat pulse, and final series of magnetizations, all performed with the ^{3}He temperature regulated, the regulation was stopped by closing the ^{4}He pressure line between the external pressure bomb and the cryostat. Thus the temperature of the cell was allowed slowly to rise in response to the heat leak present. In a two-hour period the temperature rose from 2.5 mK to 3.7 mK and magnetizations were recorded at three to five minute intervals.

NOTES

1 This possibility was pointed out by W.P. Halperin, D.D. Osheroff and H. Meyer at the 1977 Sanibel Symposium.

2 The gravitationally induced pressure differential gives rise to a temperature gradient of only 5 μK/cm.

CHAPTER IV

RESULTS AND CONCLUSIONS

Exchange Parameters Extracted from Pressure Data

Shown in Figure 10 are the pressure data for a sample of solid ^{3}He with molar volume V = 23.96 cm^3/mole as measured with the thinner diaphragm. The effect of the applied field is readily seen to be one of lowering the exchange pressure. From Eqn. (1.11) we see that a decrease in pressure with increasing field requires that J_{xzz}/k be negative indicating that antiferromagnetic ordering is to be expected. The dashed curve with no data points indicated is the calculated behavior for a field B = 4.9 T using the HNN model with a value of J determined from the B = 0 data. The measured behavior in a field of 4.9 T is shown as the inverted triangles. It is evident that the pressure effect caused by the magnetic field is about half that predicted by the HNN model.

Again referring to Eqn. (1.11) we see that a plot of P versus 1/T in zero field should be a straight line with slope equal to

$$\frac{3}{2}\frac{Nk}{V}\gamma_{xx}\left(\frac{J_{xx}}{k}\right)^2 . \qquad (4.1)$$

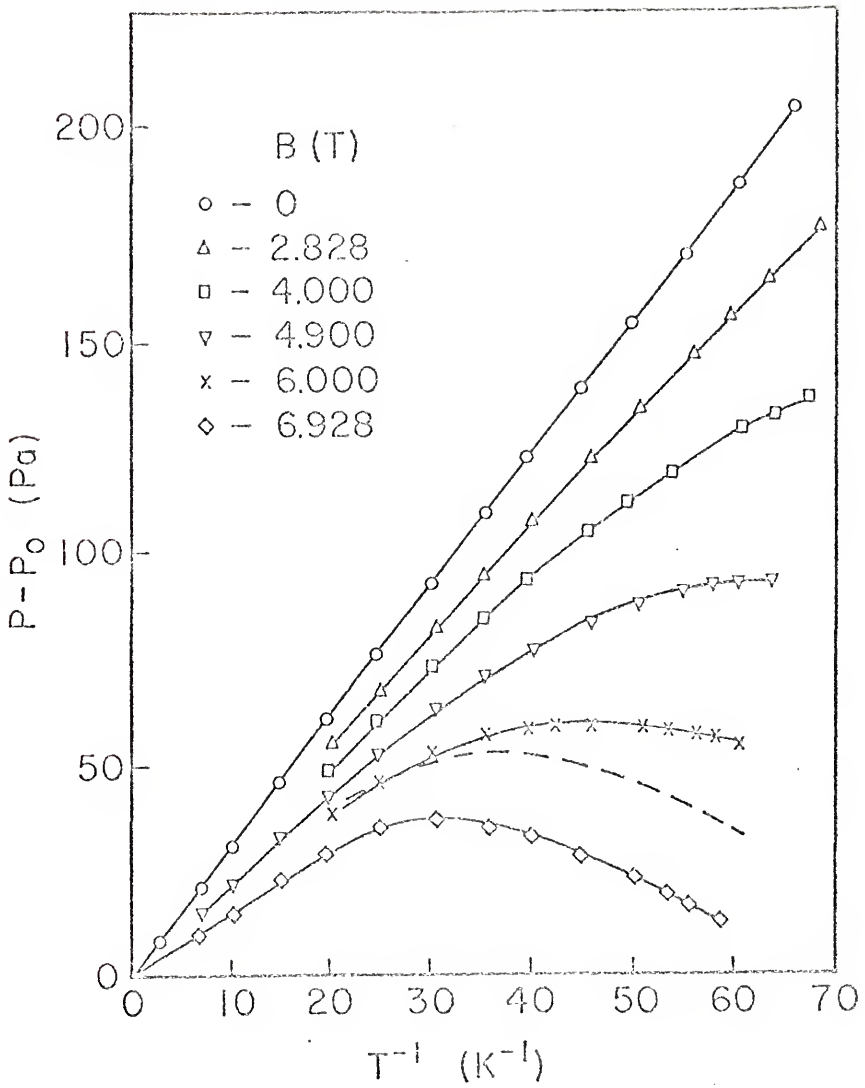

Fig. 10 Pressure Change with Temperature for Various Fields.

Pressure scale has not been corrected to account for non-constant cell volume.

As discussed previously, the pressures measured were lowered substantially by the nonconstant volume of the cell. We must multiply the pressure scale by the factor 2.50 (as determined in the previous chapter) to arrive at the constant-volume pressure. When this is done, we find the slope to be 7.74 PaK. Using a value of γ_{xx} of 35 as is suitable for a molar volume of 23.96 cm^3/mole (note that $\gamma_{xx} = 2\partial\ell n|J|/\partial\ell nV$), we calculate a value of $J_{xx}/k = 0.65$ mK. This value is in good agreement with those found in other pressure measurements (Panczyk and Adams, 1969) and also in specific heat measurements (Castles and Adams, 1973 and Greywall, 1977). The specific heat measurement of Dundon and Goodkind yield a value approximately 25% larger than this.

For a quantitative measure of the magnetic field dependence of the pressure we have plotted the data in Figure 11 as the change in pressure produced by the applied field, P(T,0) - P(T,B), versus the applied field squared. The straight lines that result for each temperature are confirmation of the B^2 dependence. A value of J_{xzz}/k can be calculated from Eqn. (1.11) by noting that the slopes of these lines are given by

$$\frac{2N_{II}^2}{VkT^2}\gamma_{xzz}\left(\frac{J_{xzz}}{k}\right) . \qquad (4.2)$$

The slope of the 1/T = 60 data is 8.93 Pa/T^2 after the correction for constant volume pressure has been applied. The value $\gamma_{xzz} = 17.5$ is used as deduced by Guyer (1977) from

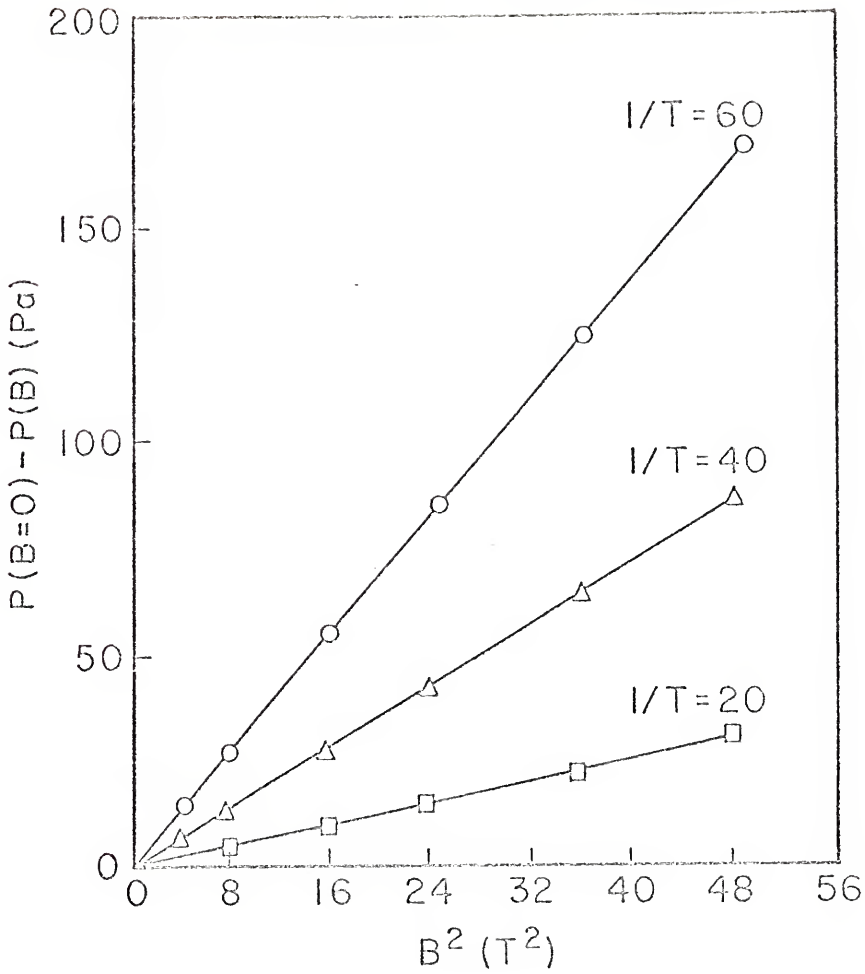

Fig. 11 Field Dependence of the exchange pressure.

Pressure scale has not been corrected to account for non-constant cell volume.

the data of Kirk and Adams (1971,1974). Thus J_{xzz}/k is determined to be -0.34 mK. The other 1/T data yield the same result verifying the $1/T^2$ dependence (see Eqn. (1.11)) of the pressure shift caused by the applied field. We therefore find a value of J_{xzz} about half the value of J_{xx}, in agreement with Kirk and Adams and in strong disagreement with the HNN model.

The major source of error in determining these two exchange constants is in the scale factor applied to the pressure in order to correct for the nonconstant volume of the cell. Values used for the compressibility of solid ^{3}He used in Eqn. (3.2) for the two diaphragms were taken from Straty and Adams (1968) and are estimated to be accurate to about 2%. The accuracy of the dV/dP determinations discussed in the previous chapter for each cell is about 3%. The "effective volume" V of the cell involves subtracting the products of these terms and hence has an estimated error on the order of 10%.

A more precise statement of the results may be made by eliminating the effect of the pressure correction. The ratio $(J_{xx}/k)^2/(J_{xzz}/k)$ is independent of the pressure scale and is equal to 1.24 mK. The accuracy of this ratio is essentially limited to the accuracy of γ_{xx} and γ_{xzz}.

Guyer (1977) uses a value of γ_{xzz} equal to one half γ_{xx}, based on assumed similar molar volume dependence (recall $\gamma_{xzz} = \partial \ln|J_{xzz}|/\partial V$ while $\gamma_{xx} = 2\partial \ln|J_{xx}|/\partial V$) and the measurements of Kirk and Adams (1971) over a somewhat limited range

of molar volumes. We must also note that the magnetic field dependence of these data had a rather large scatter thus indicating that the value $\gamma_{xzz} = \gamma_{xx}/2$ could be the source of substantial errors. By leaving the values of γ_{xx} and γ_{xzz} unspecified the results can be stated as $[\gamma_{xx}/\gamma_{xzz}](J_{xx}/k)^2/(J_{xzz}/k) = 2.48$ mK which entails experimental error whose major contribution is the molar volume determination. This error is less than 2%.

The value of $J_{xzz} = -0.34$ mK reported here is well within the error bars of the Kirk and Adams results shown in Table 1 and the reduction in uncertainty is significant.

Magnetic Susceptibility

Results of the magnetization measurements are shown in Figure 12 with χ^{-1} plotted versus T. For temperatures of 4 mK and higher the data can be represented reasonably well by a Curie-Weiss law $\chi = C/(T-\theta)$ with θ equal aboout -3.7 mK. Below 4 mK a marked increase in χ above the Curie-Weiss value is observed. In the temperature interval from 4 mK to 2.5 mK the increase in χ is so rapid that a plot of inverse susceptibility would extrapolate to a positive intersection with the T axis. Such behavior as is shown in this region would be expected to occur in a system approaching a ferromagnetic region, but the susceptibility does not rise higher than the Curie law. Below 2.5 mK the inverse susceptibility again extrapolates to a negative intercept this time with an intercept of approximately -2 mK rather than the previous -3.7 mK.

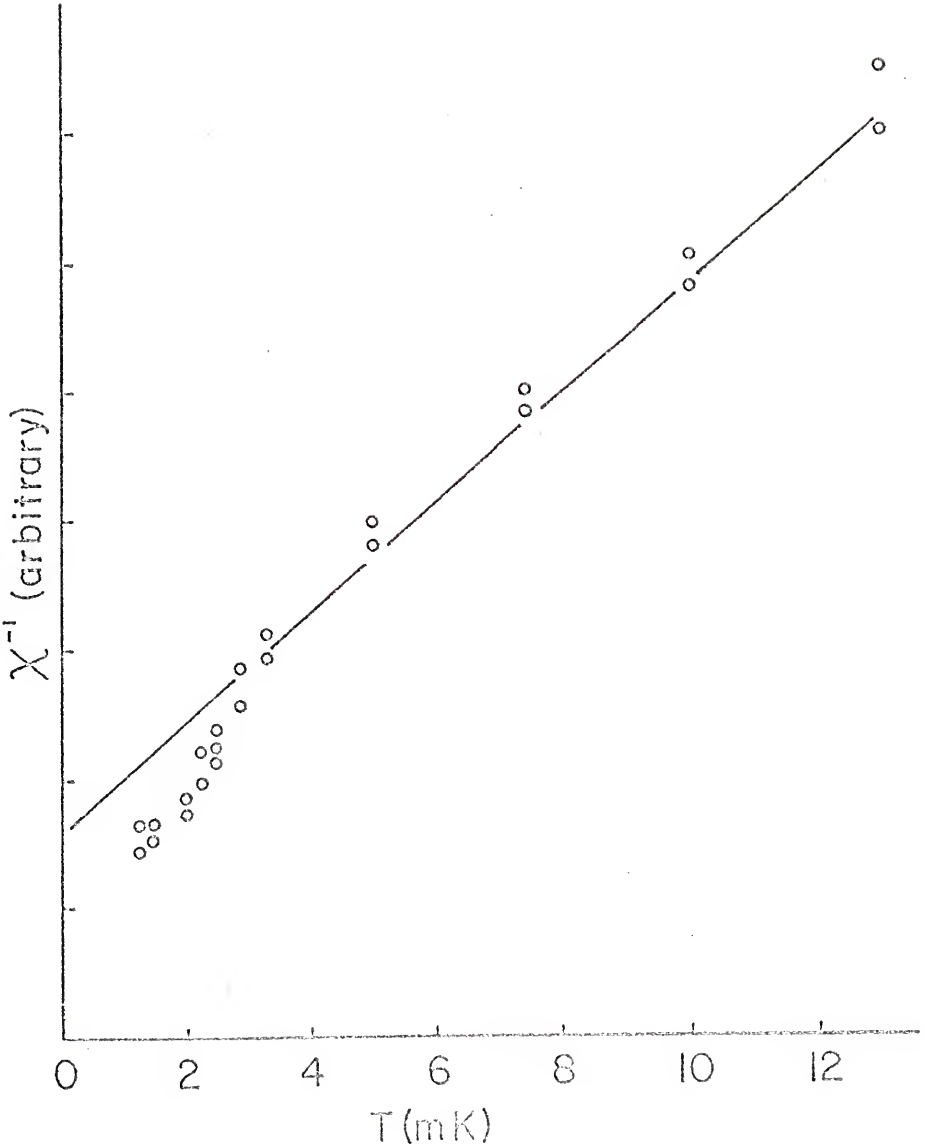

Fig. 12 Curie-Weiss plot of solid Helium three inverse susceptibility.

As mentioned earlier, this method of plotting susceptibilities is quite subject to errors in extrapolating to find the T axis intercept. Higher order terms in Eqn. (1.12) produce curvature which can be quite pronounced at these low temperatures and can lead to an overestimate of the magnitude of the intercept. In an effort to account for these higher order terms a plot of χT versus $1/T$ is shown in Figure 13. Also shown on this plot are susceptibilities calculated from the high-temperature expansion of the HNN model for various values of J. These curves are calculated using the ten coefficients given by Baker et al. We see that at the higher temperatures the data can be fitted equally well by the curves for $J/k = -0.4$ mK and for $J/k = -0.6$ mK, still in conflict with the pressure measurement determination of $J_{xzz}/k = -0.34$ mK. This could be because the inadequacy of the HNN expansion for J_{xzz} or could be a result of the lack of convergence for this number of terms at these temperatures. The low temperature data on this plot are also interesting. A negative slope indicates an approaching antiferromagnetic transition (negative Weiss theta) and a postive slope indicates a positive Weiss theta. The positive slope seen between $1/T = 250$ and $1/T = 400$ corresponds to the rapid drop in $1/\chi$ between 4 mK and 2.5 mK. This feature seems to be reproducible. It was evident in both sets of data, each taken with a different NMR coil geometry in an attempt to localize the rf pulse. As another check on the behavior in this temperature interval the magnetization was monitored at

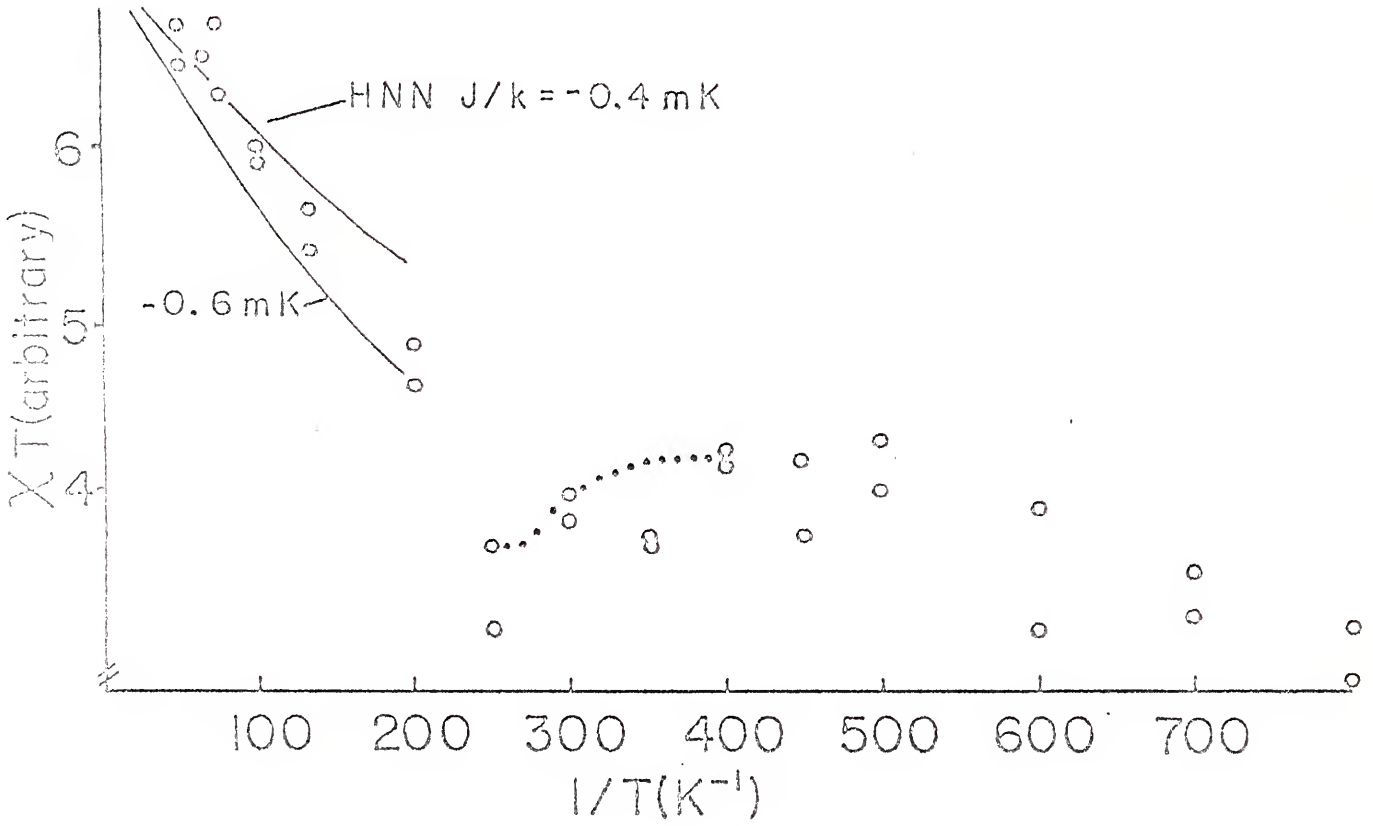

Fig. 13 χT plot of solid Helium three susceptibility.

Open points are heat-pulse data, closed points are data taken while drifting up in temperature.

three to five minute intervals while the temperature drifted from 2.5 mK up to 3.7 mK (without heat pulses, as explained in the previous chapter). As the temperature crossed the superfluid A transition the magnetization increased, corresponding to the magnetization of the normal liquid. The size of this step agreed closely with the magnetization of the liquid measured at 20 mK with no solid present. Magnetizations of the solid measured during this period of drifting temperature followed the same temperature dependence as did the susceptibilities recorded in the usual manner, indicating that the amount of solid in the NMR region was quite constant. Thus although solid was being formed as the cell warmed, it was undoubtedly accumulating in the upper portion of the Pomeranchuk cell rather than in the tail section.

Further confirmation of this unusual behavior would be desirable.

Other investigators have recently reported qualitatively similar susceptibility results. Bernier and Delrieu (1977) using a spin echo technique find an increase in susceptibility above the Curie-Weiss law at temperatures below 4 mK. Prewitt and Goodkind (1977) have measured the susceptibility of solid cooled by nuclear demagnetization of copper and also find the same deviation from the Curie-Weiss law. They also report a sharp drop in susceptibility seen to occur at 1.35 mK which they are unable to explain by means of a simple two sub-lattice model. Morii et al. (1977) also report

measurements performed in a Pomeranchuk cell showing a similar increase in susceptibility over the expected results.

It should be noted that since the present susceptibility measurements were performed on thin layers of solid in thermal equilibrium with liquid, the possibility of a process peculiar to the interface influencing the results must be considered. Ahonen et al. (1976,1977) have measured the susceptibility of ^{3}He liquid in geometries with large surface areas and found pronounced ferromagnetic behavior at temperatures below 2 mK. Sokoloff and Widom (1977) propose that the thin film of "solid" formed at the boundary of the liquid, undergoes a long range indirect spin coupling through exchange of atoms with the liquid. An atom in the solid can exchange with an atom of opposite spin in the liquid and at another point in the solid the process could be reversed, leaving the liquid in its original state but producing what amounts to a long range exchange interaction between atoms in the solid. Such a process can be used to explain the positive Curie-Weiss intercept observed in the liquid by Ahonen et al.

While the surface area of the solid in the experiment being presented here is considerably less than the surface area of the liquid measurements of Ahonen et al., the possibility of a mechanism such as this producing the observable effects cannot be ruled out.

The recent susceptibility measurements of Previtt and Goodkind (1977), which confirm the measurements reported

here, were performed on solid cooled without the presence of a liquid interface. This would indicate that the observed departure from the Curie-Weiss law was not produced by an effect occurring at the solid-liquid interface. However, the magnetic phase transition and specific heat anomaly observed by these investigators are reported to occur at 1.35 mK as opposed to 1.1 mK as reported by Kummer et al. and Halperin et al. If this discrepancy does not arise from an error in thermometry (such an error does seem possible), it might indicate that the transitions observed using compressional cooling are significantly affected by the existence of the solid-liquid interface.

It is also of interest to note here that both Kummer et al. and Halperin et al. calculated specific heats from their entropy measurements. While the differentiation involved reduces the accuracy of the results, it is significant that both groups found a small specific heat peak at about 3 mK and a larger peak in the specific heat at a temperature ranging from 0.4 mK to 0.8 mK above the final ordering of the solid.

Direct measurements of the specific heat of bulk solid ^{3}He cooled by nuclear demagnetization of copper by Dundon and Goodkind (1974) show similar behavior. Just below 4 mK a small peak occurs followed by a larger peak at a lower temperature but still above the final ordering temperature. The higher temperature specific heat feature occurs quite close to the rapid increase in susceptibility reported here.

Another feature of the entropy data of Kummer er al. noted by Halpern (1977) is that throughout the temperature range of 1.6 mK to 2.5 mK and for fields less than 0.8 T, the change in entropy for two given field strengths is approximately independent of temperature. From the Maxwell relation $(\partial S/\partial B)_T = (\partial M/\partial T)_B$, this implies that the magnetization is approximately linear in temperature. The present data are consistent with a linear behavior in this range of temperature, rather that the $1/(T - \theta)$ dependence of the Curie-Weiss law.

Comparison with Theoretical Efforts

Since the HNN model was first seriously brought into question, by the results of Kirk and Adams (1971), the Hamiltonian has been generalized to include various exchange mechanisms such as those listed in the initial chapter. Triple exchange was proposed by Zane (1972 a,b,c) to explain the results of Kirk and Adams but failed to explain the ordering temperature which was soon determined by Halperin et al. A similar problem was faced by the treatment of Goldstein (1973,1974). The possibility of quadruple exchange was presented by Guyer (1974) and calculations by McMahan and Wilkins (1975) showed that such an interaction could be important. Four spin exchange was used by Heatherington and Willard (1975) to produce a magnetic phase diagram similar to that found experimentally by Kummer et al. Recently Roger et al. (1977) have presented calculations showing that the

increased susceptibility below 4 mK could possibly be explained by including four-spin exchange in the Hamiltonian.

Their approach is essentially a generalization of that taken by Heatherington and Willard. The Hamiltonian of Roger et al. includes pair exhange up to third nearest neighbors and the two cyclic quadruple exchange terms mentioned previously, the folded array (F) and the planar array(P),

$$H = -2 \sum_{n=1}^{3} \left(J_n \sum_{i<j} (\vec{I}_i \cdot \vec{I}_j) \right) - 4J_{4F} \sum_{i<j<k<\ell}^{F} \mathcal{P}_{ijk\ell} - 4J_{4P} \sum_{i<j<k<\ell}^{P} \mathcal{P}_{ijk\ell} \tag{4.3}$$

where $\mathcal{P}_{ijk\ell} = (\vec{I}_i \cdot \vec{I}_j)(\vec{I}_k \cdot \vec{I}_\ell) + (\vec{I}_i \cdot \vec{I}_\ell)(\vec{I}_j \cdot \vec{I}_k) - (\vec{I}_i \cdot \vec{I}_k)(\vec{I}_j \cdot \vec{I}_\ell)$.

Only the (P) four-spin permutation involves third neighbors (the longer diagonal). Hence Roger et al. assume $J_3 = J_{4P}/2$ to simplify further calculations, such as the partition function expansion. The results are given here in the notation adopted previously in the work:

$$J_{xzz} = J_1 + \frac{3}{4} J_2 + \frac{3}{2} J_3$$

$$J_{xx}^2 = J_1^2 + \frac{3}{4} J_2^2 + \frac{3}{2} J_3^{2'} + 2.625 (J_{4F}^2 + J_{4P}^2) \ . \tag{4.4}$$

Values for J_{xzz} and J_{xx}^2 are then taken from previous experimental works. By treating J_{4F} and J_{4P} as variables, and using molecular field approximations, Roger et al. find (as did Heatherington and Willard) that the phase diagram of

Kummer et al. is produced only when J_{4F} completely predominates over J_{4P}. (This is in direct contrast with the calculations of McMahan and Wilkins who find the J_{4P} process to be much more favorable than the J_{4F} process.)

Using the parameters of Hetherington and Willard (including $J_{4P} \equiv J_3 \equiv 0$) Roger and Delrieu (1977) evaluate the leading correction to the Curie-Weiss law and find,

$$\chi^{-1}(T) = N^{-1}\,\mu^2[T - 3.12\ \text{mK} - \frac{1.7\ \text{mK}}{T} - \ldots] \ , \qquad (4.5)$$

i.e., that the magnetic susceptibility increases with respect to the Curie-Weiss law below 10 mK in agreement with the results presented here, and the early measurements of Osheroff (1972 a,b). For temperatures below about 6 mK higher order corrections are expected to be important, but Roger and Delrieu argue that the qualitative behavior should be given by this leading correction even below 6 mK.

Concluding Remarks

Measurements of the magnetic susceptibility and exchange pressure in magnetic fields have been performed for solid ^{3}He. These measurements are used to evaluate the lowest order magnetic exchange constant J_{xzz}.

The temperature and magnetic field dependence of the exchange pressure have been verified and the accuracy of J_{xzz} has been increased considerably.

Measurements of the magnetic susceptibility have been extended to temperatures approaching the ordering transition. A high temperature expansion using ten terms was used in an attempt to determine the constant J_{xzz} but the precision of the data or the lack of convergence for the expansion does not permit a precise value of J_{xzz} to be chosen.

At temperatures below 4 mK the susceptibility rises considerably above the Curie-Weiss law before returning to an antiferromagnetic behavior below 2.5 mK.

Susceptibility behavior increasing above the Curie-Weiss law has been explained through use of a Hamiltonian involving large contributions of quadruple exchange, quite similar to the Hamiltonian used to explain the magnetic phase diagram in this temperature range. These theoretical approaches are both based on a high temperature expansion of the partition function which is of questionable value as the ordering temperature is approached. A more complete understanding of the magnetic behavior of ^{3}He will depend on more general theoretical approaches as well as more extensive measurements of magnetic effects both in the ordered phase and at pressures above the melting curve.

APPENDIX A
PRESSURE DATA

Constant volume correction has not been applied.

B = 0.0 T

$1/T\ (K^{-1})$	$P - P_o$ (Pa)
6.66	25.9
10.05	34.2
15.15	48.4
19.92	64.9
24.87	79.5
30.58	97.0
35.71	113.7
40.48	125.2
46.30	142.8
51.02	156.2
56.18	171.8
57.80	205.8
60.98	190.7
66.22	210.5
70.42	220.9
75.19	236.4

B = 2.0 T

$1/T\ (K^{-1})$	$P - P_o$ (Pa)
6.66	17.2
10.05	28.6
15.15	39.2
18.73	53.6
19.92	54.0
24.87	68.7
30.58	84.0
35.71	99.8
40.48	110.7
46.30	125.5
51.02	137.8
54.94	150.5
56.18	152.0
60.98	167.8
66.22	179.8
70.42	193.0
71.94	198.9

B = 2.8 T

$1/T\ (K^{-1})$	$P - P_o$ (Pa)
6.66	19.6
10.05	24.3
15.15	40.4
19.92	55.0
24.87	68.4
30.58	84.2
35.71	96.7
40.48	108.1
46.30	121.3
50.63	130.0
51.02	133.8
56.18	145.6
57.80	147.5
58.82	151.2
66.00	169.7
67.34	174.4
68.03	175.6
68.49	177.9

B = 4.0 T

$1/T\ (K^{-1})$	$P - P_o$ (Pa)
6.66	16.5
10.31	22.9
16.00	35.6
19.72	46.7
24.81	63.2
30.58	69.8
35.71	85.0
40.48	92.5
46.08	105.2
49.75	110.2
54.35	116.8
60.98	130.7
62.11	130.5
65.36	134.0
66.67	135.9

B = 4.9 T

$1/T\ (K^{-1})$	$P - P_o$ (Pa)
6.66	13.9
10.05	19.8
15.15	33.5
19.92	42.9
24.87	53.6
30.58	62.5
35.71	69.6
40.16	77.4
46.30	81.6
51.02	85.9
56.18	91.1
58.82	93.9
60.24	94.6
62.50	92.5
63.69	94.2

B = 6.0 T

$1/T\ (K^{-1})$	$P - P_o$ (Pa)
6.66	31.2
10.65	36.1
15.15	47.2
19.92	55.5
24.87	62.1
30.58	69.8
35.71	74.1
40.48	75.7
46.30	74.3
51.81	74.8
53.33	73.6
56.18	73.4
58.82	72.0
60.98	71.3

B = 6.9 T

$1/T\ (K^{-1})$	$P - P_o$ (Pa)
6.66	10.4
10.05	14.2
15.15	22.2
19.92	28.6
24.87	35.2
30.58	35.9
35.71	34.7
40.48	33.0
46.30	29.0
51.02	22.6
53.19	18.9
54.35	18.4
56.18	16.5
58.48	13.4

APPENDIX B
SUSCEPTIBILITY DATA

Heat-pulse Method

T (mK)	χ (Arbitrary Units)
1.25	2720.4
	2440.3
1.43	2620.5
	2430.5
1.66	2498.8
	2035.8
2.00	2310.6
	2136.0
	2103.9
2.22	2018.2
	1794.0
2.50	1855.3
	1825.0
	1816.0
2.86	1544.6
	1392.9
	1386.1
3.33	1223.0
	1181.8
	1179.0
4.00	977.9
	867.4
	842.6
5.00	946.1
	888.7
	859.6
7.50	822.3
	794.2

T (mK)	χ (Arbitrary Units)
10.00	686.8
	659.7
	648.0
13.00	569.8
	532.35
15.00	477.7
	475.7
20.00	400.9
	374.2
	367.2

Drifting Up In Temperature

T (mK)	χ (Arbitrary Units)
2.53	1803.4
2.62	1796.8
2.67	1766.5
2.71	1744.3
2.73	1710.9
2.84	1652.1
2.88	1591.8
2.94	1542.5
2.98	1489.8
3.03	1447.2
3.09	1385.6
3.14	1344.9
3.19	1306.8
3.23	1266.7
3.28	1241.0
3.33	1197.6
3.37	1173.3
3.41	1125.0
3.45	1105.2
3.50	1076.0
3.54	1049.2
3.58	1033.4
3.62	1006.0
3.66	994.4
3.71	971.0

APPENDIX C
THERMAL TIME CONSTANT CALCULATIONS

In the heat-pulse experiments discussed here thermal equilibrium occurred within approximately 10 seconds of the heat-pulse application. This implies a thermal time constant on the order of three seconds for a layer of solid ^{3}He with a thickness of a few microns (approximately 1 μm thickness per heat-pulse).

Johnson and Wheatley (1970) report an exchange diffusion constant, D, equal to 1.2×10^{-11} m^2/sec for solid formed in a Pomeranchuk cell below 10 mK. From this value we may calculate a time constant

$$\tau = \frac{\ell^2}{D} = 0.75 \text{ sec}$$

for a layer of 3 μm thickness.

Another approach to calculating the thermal time constant is to consider the specific heat and thermal conductivity measured at higher temperatures with a suitable extrapolation applied for the low temperatures. The molar specific heat of solid ^{3}He near melting has been measured quite accurately down to 40 mK by Greywall (1977). A T^{-2} extrapolation to 2 mK yields a specific heat value of 4 J/mole K. The thermal conductivity of solid ^{3}He has been measured by Bertman, Fairbank, White and Crooks (1966) to be approximately 2 W/K m at 400 mK which may be extrapolated to 5×10^{-7} W/K m at 2 mK using a T^{-3} temperature dependence. For a molar volume, v, near melting we have

$$\tau = \frac{\ell^2 C}{k\ v} = 2.9 \text{ sec}$$

for a thickness of 3 μm.

While the close agreement of this latter calculation with our observed time constant is probably fortuitous, we can safely say that neither approach seriously questions the reasonableness of our 10 second equilibrium time.

REFERENCES

Adams, E.D., G.C. Straty, and E.L. Wall, 1965, Phys. Rev. Lett. 15, 549.

_____ , and L.H. Nosonow, 1973, J. Low Temp. Phys., 11, 11.

Ahonen, A.I., T. Kodama, M. Krusius, M.A. Paalanen, R.C. Richardson, W. Schoepe, and Y. Takano, 1976, J. Phys. C 9, 1665.

_____ , J. Kokko, O.V. Lounasmaa, M.A. Paalanen, R.C. Richardson, W. Schoepe, and Y. Takano, 1977, in Proceedings of the Second International Symposium on Quantum Fluids and Solids held on Sanibel Island, edited by S.B. Trickey, E.D. Adams, and J.W. Dufty (Plenum, New York), p. 171.

Bakalyar, D.M., C.V. Britton, E.D. Adams, and Y.-C. Hwang, 1977, Phys. Lett. to be published.

Baker,Jr., G.A., H.E. Gilbert, J. Eve, and G.S. Rushbrooke, 1967, Phys. Rev. 164, 800.

Bernandes, N., and H. Primakoff, 1960, Phys. Rev. 119, 968.

Bernat, T.P. and H.D. Cohen, 1973, Phys.Rev. A 1, 1709.

Bernier, M., and J.M. Delrieu, 1977, Phys. Lett. 60A, 156.

Bertman, B., H.A. Fairbank, C.W. White, and M.J. Crooks, 1966, Phys. Rev. 142, 74.

Castles, S.H., and E.D. Adams, 1973, Phys. Rev. Lett. 30, 1125.

_____ , and E.D. Adams,1975, J. Low Temp. Phys. 19, 397.

Dundon, J.M., and J.M. Goodkind, 1974, Phys. Rev. Lett. 32, 1343.

Flint,E.B., E.D. Adams, and C.V. Britton, 1977, in Proceedings of the Second International Symposium on Quantum Fluids and Solids held on Sanibel Island, edited by S.B. Trickey, E D. Adams, and J.W. Dufty (Plenum, New York), p. 337.

Goldstein, L., 1973, Phys. Rev. A 8, 2160.

_____ , 1974, J. Low Temp. Phys. 15, 583.

Greywall, D.S., 1977, Phys. Rev. B 15, 2604.

Guyer, R.A., R.C. Richardson, and L.T. Zane, 1971, Rev. Mod. Phys. 43, 532.

_____ , 1974, Phys. Rev. a 9, 1452.

_____ , 1977, J. Low Temp. Phys., to be published.

Halperin, W.P., C.N. Archie, F.B. Rasmussen, R.A. Buhrman, and R.C. Richardson, 1974, Phys. Rev. Lett. 32, 927.

_____ , C.N. Archie, F.B. Rasmussen, and R.C. Richardson, 1975, Phys. Rev. Lett. 34, 718.

_____ , 1977, Proceedings of the International Quantum Crystal Conference held at Colorado State University, unpublished.

Heatherington, J.H., and F.D.C. Willard, 1975, Phys. Rev. Lett. 35, 1442.

Johnson, R.T., and J.C. Wheatley, 1970, J. Low Temp. Phys. 2, 423.

Kirk, W.P., E.B. Osgood, and M. Garber, 1969, Phys. Rev. Lett. 23, 833.

_____ , and E.D. Adams, 1971, Phys. Rev. Lett. 27,392.

_____ , and E.D. Adams, 1974, in Low Temperature Physics - LT13, edited by K.D. Timmerhaus, W.J. O'Sullivan, and E.F. Hammel (Plenum, New York), Vol. 2, p. 149.

Kummer, R.B., E.D. Adams, W.P. Kirk, A.S. Greenberg, R.M. Mueller, C.V. Britton, and D.M. Lee, 1975, Phys. Rev. Lett. 34, 517.

_____ , R.M. Mueller, and E.D. Adams, 1977, J. Low Temp. Phys. 27, 319.

McMahan, A.K., and R.A. Guyer, 1973, Phys. Rev. A 7, 1105.

_____ , 1974, Quantum Solids and Fluids; CAP International Summer School in Theoretical Physics; Kimberley, Ontario, unpublished.

_____ , and J.W. Wilkins, 1975, Phys. Rev. Lett. 35, 376.

Morii, Y., K. Ichikawa, T. Hata, C. Kanamori, H. Okamoto, T. Kodama, and T. Shigi, to be published.

Osheroff, D.D., 1972a, Ph.D. dissertation, Cornell Univ.

_____ , R.C. Richardson, and D.M. Lee, 1972b, Phys. Rev. Lett. 28, 885.

Panczyk, M.F., R.A. Scribner, G.C. Straty, and E.D. Adams, 1967, Phys. Rev. Lett. 19, 1102.

_____ , and E.D. Adams, 1969, Phys. Rev. 187, 321.

Pipes, P.B., and W.M. Fairbank, 1969, Phys. Rev. Lett. 23, 520.

Pomeranchuk, I.I., 1950, Zhur. Eksp. i. Theoret. Fiz. 20, 919.

Prewitt, T.C., and J.M. Goodkind, 1977, Proceedings of the International Quantum Crystal Conference held at Colorado State University, unpublished.

Ramm, H., P. Pedroni, J.R. Thomnson, and H. Meyer, 1970, J. Low Temp. Phys. 2, 539.

Richardson, R.C., E. Hunt, and H. Meyer, 1965, Phys. Rev. A 138, 1326.

Roger, M., J.M. Delrieu, and A. Landesman, 1977, Phys. Lett., to be published.

_____ , and J.M. Delrieu, 1977, preprint, to be published.

Sites, J.R., D.D. Osheroff, R.C. Richardson, and D.M. Lee, 1969, Phys. Rev. Lett. 23, 836.

Sokoloff, J.B., and A. Widom, 1977, Proceedings of the International Quantum Crystal Conference held at Colorado State University, unpublished.

Straty, G.C., and E.D. Adams, 1967, Phys. Rev. 169, 232.

_____ , and E.D. Adams, 1969, Rev. Sci. Instr. 40, 1393.

Trickey, S.B., W.P. Kirk, and E.D. Adams, 1972, Rev. Mod. Phys. 44, 668.

Zane, L.I., 1972a, Phys. Rev. Lett. 28, 420.

_____ , 1972b, J. Low Temp. Phys. 9, 219.

_____ , 1972c, Phys. Lett. 41A, 421.

_____ , and J.R. Sites, 1974, J. Low Temp. Phys. 17, 159.

BIOGRAPHICAL SKETCH

Charles Valentine Britton was born on January 18, 1947 in Kingsport, Tennessee, where he graduated from Dobyns-Bennett High School in June, 1965. He then entered Duke University in Durham, North Carolina, was elected into Sigma Pi Sigma, physics honor society, and received the Bachelor of Science degree in physics in June, 1969. He began graduate studies at the University of Florida in September of that year. Following service in the United States Army from Sept. 1970 until June 1972 he has been pursuing the Doctor of Philosophy Degree at the University of Florida. He is married to the former Rose Patryce Guthrie and is the father of a nine-year-old daughter, Rose Patryce.

I certify that I have read this study and that in my opinion it conforms to acceptable standards of scholarly presentation and is fully adequate, in scope and quality, as a dissertation for the degree of Doctor of Philosophy.

E. Dwight Adams

E. Dwight Adams, Chairman
Professor of Physics

I certify that I have read this study and that in my opinion it conforms to acceptable standards of scholarly presentation and is fully adequate, in scope and quality, as a dissertation for the degree of Doctor of Philosophy.

James W. Dufty

James W. Dufty
Associate Professor of Physics

I certify that I have read this study and that in my opinion it conforms to acceptable standards of scholarly presentation and is fully adequate, in scope and quality, as a dissertation for the degree of Doctor of Philosophy.

Gary G. Ihas

Gary G. Ihas
Assistant Professor of Physics

I certify that I have read this study and that in my opinion it conforms to acceptable standards of scholarly presentation and is fully adequate, in scope and quality, as a dissertation for the degree of Doctor of Philosophy.

Robert R. Kallman

Robert R. Kallman
Professor of Mathematics

I certify that I have read this study and that in my opinion it conforms to acceptable standards of scholarly presentation and is fully adequate, in scope and quality, as a dissertation for the degree of Doctor of Philosophy.

Thomas A. Scott
Professor of Physics

This dissertation was submitted to the Graduate Faculty of the Department of Physics in the College of Arts and Sciences and to the Graduate Council, and was accepted as partial fulfillment of the requirements for the degree of Doctor of Philosophy.

December 1977

Dean, Graduate School